

N71-22870

NASA CR-111856

THE PERKIN-ELMER CORPORATION  
AEROSPACE DIVISION  
2855 Metropolitan Place, Pomona, California 91767

FINAL REPORT  
ION PUMP  
VOLUME 2 OF 6  
COMBINED STUDY PROGRAM

By N. Ierokomos

March 1971

Contract NAS1-9469  
SPO Number 30006

**CASE FILE  
COPY**

Prepared for  
NATIONAL AERONAUTICS AND SPACE ADMINISTRATION  
LANGLEY RESEARCH CENTER

Langley Station  
Hampton, Virginia 23365

THE PERKIN-ELMER CORPORATION  
AEROSPACE DIVISION  
2855 Metropolitan Place, Pomona, California 91767

FINAL REPORT  
ION PUMP  
VOLUME 2 OF 6  
COMBINED STUDY PROGRAM

By N. Ierokomos

March 1971

Prepared By N. Ierokomos Date 29 March 71  
N. Ierokomos, Project Engineer  
Approved By B.F. Bicksler Date 5/29/71  
B.F. Bicksler, Project Manager  
Approved By M.R. Ruecker Date 29 MAR '71  
M.R. Ruecker, Manager Space Physics  
Approved By W.C. Qua Date 29 Mar 71  
W.C. Qua, Program Manager

Contract NAS1-9469  
SPO Number 30006

Prepared for  
NATIONAL AERONAUTICS AND SPACE ADMINISTRATION  
LANGLEY RESEARCH CENTER  
Langley Station  
Hampton, Virginia 23365

## ABSTRACT

A program was conducted in which an instrument system concept was studied to optimize the application of a mass spectrometer as a sensor for monitoring the primary atmospheric constituents, as well as atmospheric contaminants, on board a manned spacecraft. The program was divided into six individual studies representing the primary system parts complementing the spectrometer: A Carbon Monoxide Accumulator Cell (Volume 1), an Ion Pump (Volume 2), an Ion Pump Power Supply (Volume 3), an Inlet Leak (Volume 4), an Ion Source (Volume 5), and an Undersea Atmospheric Analyzer (Volume 6). The principle goal of the combined study program was the achievement of an instrument concept of minimum power, weight and size without compromising the minimum detection limits of the instrument.

## TABLE OF CONTENTS

	<u>Page</u>
ABSTRACT	ii
SUMMARY	1
ION PUMP DESIGN	1
SUMMARY	1
Introduction	1
Results of Previous Ion Pump Analysis	2
Comparison of the Two Approaches	6
Test Results of the Varian Two Liter Per Second Pump	7
Four Liter Per Second Prototype Pump	9
Eight Cell Prototype	17
ROUGH PUMPING	20
Vacuum Line to Space	21
Cryo-Sorption Pumping	23
Sublimation Pumping	27
CONCLUSIONS	28
APPENDIX A - MAGNET DESIGN CRITERIA	30

## LIST OF TABLES

	<u>Page</u>
1. Ion Pump Comparison	7
2. Pumping Speed Test for Varian Two Liter Per Second Ion Pump (By the Two Gauge Method)	8
3. Magnetic Field Strength	11
4. Low Pressure Starting Data	12
5. High Pressure Starting Data	13
6. Current-Voltage Versus Pressure	13
7. Long Term Ion Pump Test	19
8. Pump Power Supply Behavior	20



## LIST OF TABLES (Cont)

	<u>Page</u>
9. Cryo-Sorption Pumping at 25°C	25
10. Cryo-Sorption Pumping at 0°C	26
11. Cryo-Sorption Pumping at Dry Ice Temperature	26
12. Ion Pump Comparison	29

## LIST OF FIGURES

	<u>Page</u>
1. Closed Ring Magnetic Circuit	32
2. Varian Two Liter Per Second Ion Pump	32
3. Two-Cell Prototype Ion Pump	33
4. Exploded View of Prototype Ion Pump	34
5. Ion Pump Assembled (Prototype)	35
6. Magnet Geometry	36
7. Test Vacuum System	37
8. Test Results	38
9. Typical Variations of Speed (Single Cell) With Magnetic Field for Two Values of Anode Voltage	39
10. Test Results	40
11. Magnetic Field Plots	41
12. Test Data Rerun	42
13. Test Data Rerun	43
14. Pumping Speed vs Voltage	44
15. Magnetic Field Geometry Comparison	45
16. Magnetic Field Test Results (Z-Axis)	46
17. Magnetic Field Test Results (X-Axis)	47
18. Dual Separated vs Single Magnet	48
19. Argon Pumping Speed	49

## LIST OF FIGURES (Cont)

	<u>Page</u>
20. 4 $\ell$ /sec Pump After Argon Activation	50
21. Geometry and Field Strength Affect Test Data	51
22. Pumping Speed vs Field Strength	52
23. Pumping Speed vs Field Geometry	53
24. Pumping Speed vs Voltage	54
25. Anode Assembly of Eight-Cell Ion Pump	55
26. Eight-Cell Prototype Ion Pump	56
27. Pumping Speed vs Pressure Eight-Cell Pump (Prototype)	57
28. Pumping Speed vs Voltage Eight-Cell Prototype	58
29. Pressure vs Starting Voltage	59
30. Mechanical Pumping and Foreline Trap	60
31. Cryo-Sorption Pumping (Pumps at Room Temperature 25°C)	60
32. Lowest Pressure vs Temperature Cascading Cryopumps (Two)	61
33. Typical Adsorption Isotherms	62
34. Sorption of Gases by Zeolites vs Temperature (Typical)	63

THIS PAGE INTENTIONALLY LEFT BLANK

## ION PUMP DESIGN

## SUMMARY

This report covers the design, fabrication and testing of a flight configuration Ion Pump and Magnet Assembly for use in flight mass spectrometers. The required pumping speed of about four liters per second was achieved in the final configuration. This report also includes analysis of rough pumping techniques that may be utilized to pump down a flight mass spectrometer system from some high pressure (including one atmosphere) to a pressure at which the Ion Pump may be started.

The design section includes analysis of the Ion Pump development effort conducted on NASA contract NAS1-6387 and the comparison of the analysis results with an ion pump design based on a commercial two liter per second pump. Fabrication and test data covering the Ion Pump design based on the commercial pump configuration is included. The results of this design did not achieve the pumping speed required. The pump assembly was then redesigned along with the magnet and subsequent tests showed that an acceptable pumping speed of three and one-half to four liters per second was attained.

In the rough pumping investigation, several methods were analyzed. These methods included: sublimation pumping, use of a line to outer space and cryo-sorption pumping. A line to outer space or cryo-sorption pumps with thermoelectric devices or a combination of sorption and sublimation pumping are the only space usable devices that are adequate.

## Introduction

The purpose of this study effort was to develop an optimized, low-power, lightweight Ion Pump capable of attaining a pumping speed of about four liters per second for active gases over the pressure range of  $10^{-6}$  to  $10^{-5}$  torr. The design utilized the effort accomplished on NASA Contract NAS1-6387.<sup>1</sup> This previous effort was to be analyzed and compared with the concept of combining two-two liter per second pumps designed by Varian Associates.

- 
1. Two Gas Atmosphere Sensor System (Mass Spectrometer), Phase IIa - Phase IIb, Final Report, March 1969, NAS1-6387, Addendum 1, Page 277.

In addition to the design of the Ion Pump, the complete design of a lightweight magnet was undertaken. The prototype pump was tested for running and starting current, pumping as a function of pressure and anode voltage. Also, variations in operation with time were tested. After analysis and comparison of all possibilities two design approaches were considered; first, designing around a totally new concept and second, basing the design around the Varian two liter per second pump. It was decided to use the second possibility. This decision was made because of the possible risks present in a totally new concept. After extensive discussions with Varian Associates and the Ultek Division of Perkin-Elmer the totally new concept was abandoned because it involved resks due to schedule and cost unknowns. A weight analysis indicated that using the Varian two liter per second design as a basis, lightweight design could be achieved provided the magnet was completely redesigned.

### Results of Previous Ion Pump Analysis

Under NASA Contract NAS1-6387 an extensive analysis was conducted concerning the theory of operation of an ion pump. Some of the more pertinent relations and conclusions have been taken from that report and compared with expected results of the second alternative of using a modified commercial design to determine the course of action to follow. The final report for the above referenced contract shows that the maximum pumping speed, which can be obtained from any ion pump, is limited by the available receiver area with the maximum speed per unit area being

$$S_M = \sqrt{\frac{KT}{2\pi M_g}} \quad (1)$$

where:    K = Boltzman's constant  
           T = Absolute temperature  
           M<sub>g</sub> = Mass of the gas molecule

Therefore, the larger the receiver area, the higher the potential pumping speed of an ion pump. In a normal diode pump, the overwhelming part of the receiver area is the internal area of the anode. This is because any molecules absorbed or buried within the cathodes will eventually be sputtered away by the ions continually bombarding the cathodes.

A second important parameter for the determination of the pumping speed is the sputtering rate of the cathode material, which eventually can form stable compounds, with the pumped gas on the receiver surface. The pumping speed is related to the sputtering rate by:

$$S_p = c \gamma M_s I/p e \quad (2)$$

where:  $c$  = Getter capacity

$M_s$  = Mass of the sputtered atom

$\gamma$  = Coefficient of sputter yield

$e$  = Electronic charge

$I/p$  = Ion current overpressure

The two equations above show that the pumping speed is optimized by a large receiver area and a large  $I/p$  value, since the other parameters tend to be fixed by the material of the cathodes. Increasing the ion current is not a simple straightforward matter, since this current is related to the complex mechanics of the Penning discharge. The ion current resulting from a Penning discharge can be expressed by the following equation:

$$I_{ion} = PL_a r_a^2 (1 - \delta^2) / \left( \frac{1}{2S\rho \frac{e}{M_e} V_b} \right) \quad (3)$$

where:  $\rho$  = Space charge density (within anode)

$S$  = Ionization probability at  $2 V_b$

$V_b$  = Ionization potential

$P$  = Pressure

$L_a$  = length of the anode cell

$r_a$  = Radius of the anode cell

$\delta = r_k / r_a$

$r_k$  = Radius of neutral column (center of anode)

$M_e$  = Mass of electron

Equations (2) and (3) may be combined to give a general pumping speed relation for a well ordered discharge system. Giving:

$$S_p = c \gamma M_s e L_a r_a^2 (1 - \delta^2) / \left( \frac{1}{2S_p \frac{e}{M_e} V_b} \right) \quad (4)$$

Collecting all fixed terms for a given system, equation (4) may be rewritten in a geometry dependent form as:

$$S_p = K L_a r_a^2 (1 - \delta^2) \quad (5)$$

The value of  $\delta$  is strongly dependent on the applied anode voltage and magnetic field. In order, however, to derive an explicit solution of the anode voltage and current (hence pumping speed) of a Penning cell, the limiting case of the neutral column (found in the center of the anode) approaching the anode is used,

or if  $\delta \rightarrow 1$

then

$$\frac{J_v}{P} = \delta \epsilon_0 B \frac{e}{M_e} S \sqrt{V_b} \sqrt{2/3(V_a - V_k)} / r_a \quad (6)$$

where:  $\epsilon_0$  = Permittivity of free space  
 $B$  = Magnetic flux density  
 $V_k$  = Virtual cathode potential  
 $V_a$  = Anode potential

This applies until the saturation affect begins to predominate at  $\delta > 84$ .

An approximate relation of all the parameters (voltage, pressure, magnetic field, pumping speed, and geometry) may be derived by combining and rearranging equations (6) and (4) giving:

$$U_M = \frac{f_1 f_2}{H_d B_d} \left\{ \frac{4}{\pi} + 0.03 p B^2 + \frac{B^{3/4} S_p^{1/4}}{5.24} \left( \frac{\pi(1 - \delta^2)}{K_1 B r_a} \right)^{1/4} \right\} \left\{ \frac{K_1 S_p}{(1 - \delta)} \right\} \quad (7)$$

where:  $U_M$  = Volume of magnet  
 $f_1$  = Magnetomotive force (mmf) leakage factor  
 $f_2$  = Flux leakage factor  
 $H_d$  = Magnet field intensity at maximum energy  
 $B_d$  = Magnet flux density at maximum energy

$$K_1 = e / \left( 4c \delta \epsilon_0 \left( \frac{e}{M_e} \right)^{3/2} S \sqrt{V_b} \right)$$

$$\wedge = \frac{4}{\pi} \left\{ 1 + \sqrt{2} (Br_a)^{3/2} \sqrt{\frac{\pi(1 - \delta^2)}{4K_1 S_p B}} \left( \frac{4}{\pi} + 0.03PB^2 + \frac{B^{3/4} S_p}{5.24} \left( \frac{\pi(1 - \delta^2)}{K_1 Br_a} \right)^{1/4} \right) \right\}$$

In the referenced contract (NAS1-6387) the following values were calculated for the required pumping speed of four liters per second.

$B = 2500$   
 $r_a = 3/32$  in  
 $L_a = 3/8$  in  
 $n_c = 40$  cells  
 $L_{ak} = 0.04$  in  
 $V_a = 1670$  V  
 $V_k = 670$  V  
 $I/p = 65$  A/T  
 $l_M = 3.6$  in (magnet length)  
 $A_M = 0.63$  in<sup>2</sup> (magnet area)

The ion pump that was constructed under NASA Contract NAS1-6387 consisted of two sections with a closed ring magnetic circuit (Figure 1). Tests indicated, however, that the pump would not start below  $10^{-5}$  torr. The cause for not starting at low pressures, as stated in the above report, was attributed to the starting voltage being too close to the saturation value. It is now suspected that the electron radii, under the given magnetic field, were too large under the given  $r_a$  so that the electrons would hit the anode and be captured before they had a chance to ionize the gas molecules at the required rate. This is because at lower pressures the molecular density is lower. Since the electron radius is given as



$$R_e = \sqrt{\frac{E}{B}} \quad (8)$$

The solution was to increase  $Br_a$ , however, increasing  $r_a$  is easier than increasing  $B$ . An increase of  $r_a$  is also the solution for separating the starting voltage value from the saturation value. A new pump was constructed with:

$$r_a = 3/16 \text{ in}$$

$$B = 1.97 \text{ kG}$$

$$V_a = 7.5 \text{ kV}$$

$$n_c = 5 \text{ cells}$$

The above geometry (consisting of half the ion pump) gave a pumping speed of 1.34 liters per second or would have been 2.68 liters per second for the entire pump. It was stated in the above report that the pumping speed should increase by forty percent if the magnetic flux density was increased to the calculated value of 2.5 kilogauss. This statement was based on the belief that the pumping speed increases with the square of the magnetic field intensity. This is not necessarily a correct relation however, as will be shown later.

#### Comparison of the Two Approaches

During the interim, between the completion of the effort on NAS1-6387 and the initiation of the Ion Pump Study described herein, a new ion pump was developed by Varian Associates. The ion pump had a stated pumping speed of two liters per second and was small enough to be considered for possible adaptation as a flight ion pump. This ion pump was a diode type with a single cell and utilized titanium cathodes with tantalum posts situated in the center of the cathodes and projecting inward along a common centerline toward the center of the anode ring. This geometry differed radically from the one that had been investigated previously and it was therefore necessary to carefully compare the two geometries to determine which one would achieve the best operational results in a final flight configuration at four liters per second. The parameters of the two liter per second pump and those of the final tests conducted under NAS1-6387 are compared in Table 1.

TABLE 1.- ION PUMP COMPARISON

NAS1-6387 Design		2 l/sec Varian Based Design
Half Anode Assembly	Item	One - 2 l/sec Pump
1.34 l/sec	Speed	2 l/sec
1.97 kG	Mag field	1.0 kG
6 kV	Anode Voltage	3.2 kV
26 at 6 kV	I/p	18 at 3.2 kV
2 lbs	Magnet Weight	2.5 lbs (Varian) 1.5 lbs (P-E Design)
1.5 W	Power	0.65 W
0.2 in <sup>3</sup>	Max Discharge Volume	0.5 in <sup>3</sup>

The data in Table 1 shows that the Varian commercial design pump appears to have a higher pumping speed with less magnetic field and power requirements. It appears likely, therefore, that a design based on this commercial pump, with a lighter magnet, offers a higher probability of success in obtaining a pumping speed of four liters per second. Based upon this comparison it was decided to utilize the Varian design as the basis for the flight type, four liter per second ion pump. Therefore, a Varian two liter per second pump was purchased so that tests could be conducted regarding the pumping speed and other running parameters.

#### Test Results of the Varian Two Liter Per Second Pump

The commercial Varian two liter per second ion pump is of the diode configuration, consisting of two flat titanium cathodes. A tantalum post is also part of each cathode as shown in Figure 2. This post has two functions; the first function is to depress the cathode field deeper into the anode so that most of the ions will impact on this post at large angles, which enhances back scattering of neutral particles. It is presently believed that noble gases, such as argon, are pumped primarily by back scattering as neutrals which subsequently become buried in the anode by the sputtered titanium and tantalum. Increased back scattering by field depression thus causes a higher pumping speed for noble gases. For the second function the post material is tantalum, rather than titanium, because tantalum has a higher molecular weight which again improves the probability of back scattering.

This pump has an anode diameter of eight-tenths of an inch and an anode length of one inch, as shown in Figure 2. The test results indicated that the pump had a nominal pumping speed of two liters per second, as shown in Table 2. The test results indicated sufficient pumping speed for a single two liter per second pump, it was felt that two-two liter per second pumps, combined with a new magnet design, would provide a four liter per second pump.

TABLE 2.- PUMPING SPEED TEST FOR  
VARIAN TWO LITER PER SECOND ION PUMP  
(BY THE TWO GAUGE METHOD) \*

$P_1$	$P_2$	I ( $\mu$ a)	$P_1 - P_2$	$S_p$ ( $\ell$ /sec)
$3.6 \times 10^{-7}$	$8.9 \times 10^{-8}$	1.5	$2.31 \times 10^{-7}$	2.14
$2.0 \times 10^{-6}$	$3.2 \times 10^{-7}$	5.5	$1.63 \times 10^{-6}$	1.87
$5.8 \times 10^{-6}$	$8.1 \times 10^{-7}$	14	$4.9 \times 10^{-6}$	2.02
$2.1 \times 10^{-5}$	$2.8 \times 10^{-6}$	47	$1.82 \times 10^{-5}$	2.1
$5.7 \times 10^{-5}$	$8.4 \times 10^{-6}$	145	$4.86 \times 10^{-5}$	1.76
$8.7 \times 10^{-5}$	$1.4 \times 10^{-5}$	235	$7.3 \times 10^{-5}$	1.26
After System Bakeout Overnight				
$1.0 \times 10^{-6}$	$1.8 \times 10^{-7}$	2.7	$5.3 \times 10^{-7}$	1.78
$5.5 \times 10^{-6}$	$7.7 \times 10^{-7}$	12	$4.54 \times 10^{-6}$	1.67
$2.3 \times 10^{-5}$	$3.2 \times 10^{-6}$	49	$1.95 \times 10^{-5}$	1.95
$4.9 \times 10^{-5}$	$7.1 \times 10^{-6}$	113	$4.16 \times 10^{-5}$	1.8
$9.0 \times 10^{-5}$	$1.4 \times 10^{-5}$	220	$7.57 \times 10^{-5}$	1.62

\*See Page 11 for a description of the two gauge method of flow measurement.

## Four Liter Per Second Prototype Pump

To make a four liter per second pump the anode and post geometry was left identical to the two liter per second pump along with the cathode to anode spacings and the titanium cathode thickness, but two anodes were contained within a single housing, as shown in Figures 3, 4 and 5.

The anodes are separated by 0.325 inch by the supporting bracket, which in turn is supported by a 0.250 inch diameter shaft passing through the high voltage feedthrough. The shaft, in addition to providing support for the anodes, also carries the high voltage required for the pump to function. The high voltage feedthrough is a brazed ceramic insulator with a corona discharge level of over 5,800 volts.

Ion shielding, to prevent the ceramic from charging up or being contaminated, is provided by the ring shield on the supporting shaft. The entire ion pump with the exception of the cathodes and ceramic insulator is constructed from 304 CRES. To keep the geometry of this pump the same as the two liter per second commercial pump, and also provide noble gas pumping, the tantalum posts were also retained. The mechanical support was examined to insure that the resonant frequency of the anode assembly was above the 2000 hertz minimum normally required for flight applications. The computations are shown below:

The spring constant, K, of a system is defined as:

$$K = \frac{P}{y} = \frac{3EI}{L^3} \quad (9)$$

where: P = Load

y = Displacement

E = Modulus of elasticity of the support member

I = Moment of inertia

L = Length of support member

The frequency is given by:

$$f = 1/2 \pi \sqrt{\frac{K}{M}} \quad (10)$$

where:  $M$  = Mass (total)

The total mass is:

$$M = \frac{W}{g} = \frac{\text{Weight of Shaft} + \text{Weight of Anodes}}{\text{Gravitational Constant}}$$

with anode weight being

$$W_a = pV = (0.29)(0.064) = 0.0175 \text{ lbs}$$

where:  $p$  = Density

$V$  = Volume

The post weight (shaft + bracket)

$$W_p = (0.29)(0.0437) = 0.0127 \text{ lbs}$$

$$\text{thus: } M = \frac{(0.0127 + 0.0175)}{386} = 78.3 \times 10^{-6} \frac{\text{lb/sec}^2}{\text{in}}$$

$$\text{giving } K = \frac{(3)(29 \times 10^6)(191.4 \times 10^{-6})}{(0.75)^3} = 39,500 \text{ lb/in}$$

which gives a resonant frequency of:

$$f = \frac{1}{2\pi} \sqrt{\frac{39,500}{78.3 \times 10^{-6}}} = 3,580 \text{ Hz}$$

The above resonant frequency is acceptable since it is well above the 2000 hertz minimal normally specified.

Analysis of the new magnet design indicated that the field strength at the center of the air gap would be about 1200 gauss. The geometry of the magnet is shown in Figure 6. The magnet calculations are presented in Appendix A.

The pump was assembled and the magnet was charged with the magnetic field strength obtained, as a function of the changing level of the magnet charger (Model 2470-350, RFL Industries, Inc.), as shown in Table 3.

TABLE 3.- MAGNETIC FIELD STRENGTH

Charging Level (Volts)	B Field (Gauss)
1 (~70)	470
2 (~110)	1,100
3 (~150)	1,350
4 (~190)	1,390
5 (~235)	1,420
6 (~250)	1,420
7 (~300)	1,420

The magnetic field was stabilized at the designed level of 1,200 gauss and the magnet was then ready to be assembled with the ion pump. The pump assembly was installed on a vacuum system as shown in Figure 7 and baked to about 400 degrees centigrade for twenty-four hours (without the magnet).

The test vacuum system configuration allows the measurement of the pumping speed of a pump by the two gauge, known conductance method.

The pumping speed may be calculated using the general equation:

$$S_p = c \frac{\Delta P_2 - \Delta P_1}{\Delta P_1} \quad (11)$$

where:  $c$  = Known conductance

$\Delta P_2$  = Pressure reading at gauge No. 2 minus background pressure of gauge No. 2

$\Delta P_1$  = Pressure reading at gauge No. 1 minus background pressure of gauge No. 1

The background pressures are measured prior to opening the variable leak valve.

The conductance of  $c$  above is calculated from the orifice geometry:

$$c = 11.6 A \text{ } \ell/\text{sec (for } N_2) \quad (12)$$

where:  $A$  = Area of aperture in  $\text{cm}^2$

After the system was baked and the magnet was mated with the ion pump, tests to determine the starting characteristics were undertaken. With the bypass valve open and a background pressure of  $6 \times 10^{-9}$  torr the ion pump was started. The pump started with the running parameters for the low pressure start shown in Table 4.

TABLE 4.- LOW PRESSURE STARTING DATA

Time	$I_{\text{pump}}$ ( $\mu\text{A}$ )	$V_{\text{pump}}$ (Volts)	$P_1$ - torr - $P_2$	
Start	170	3,525	$6.6 \times 10^{-9}$	$6.5 \times 10^{-9}$
60 sec	140	3,525	$3.0 \times 10^{-8}$	$2.6 \times 10^{-8}$
120 sec	150	3,500	$2.6 \times 10^{-8}$	$2.3 \times 10^{-8}$
180 sec	140	3,525	$7.5 \times 10^{-8}$	$7.2 \times 10^{-8}$
240 sec	140	3,525	$2.0 \times 10^{-7}$	$1.8 \times 10^{-7}$
300 sec	135	3,525	$1.4 \times 10^{-7}$	$1.2 \times 10^{-7}$
10 min	150	3,525	$4.4 \times 10^{-8}$	$4.2 \times 10^{-8}$
15 min	125	3,525	$2.8 \times 10^{-8}$	$2.7 \times 10^{-8}$
20 min	118	3,540	$2.1 \times 10^{-8}$	$2.0 \times 10^{-8}$
25 min	115	3,540	$1.7 \times 10^{-8}$	$1.6 \times 10^{-8}$
30 min	115	3,540	$1.6 \times 10^{-8}$	$1.6 \times 10^{-8}$

Having shown that the pump is capable of starting successfully at very low pressures, testing with high pressure starts were initiated. The high pressure tests were conducted by turning the pump off, closing the bypass valve and opening the variable leak until the desired pressure was attained. The test gas in all cases was nitrogen. The high pressure starting conditions are shown in Table 5.

TABLE 5.- HIGH PRESSURE STARTING DATA

$P_1$ (torr)	$V_p$ (volts)	$I_p$
$1.0 \times 10^{-3}$	3,480	520 $\mu$ A
$5.0 \times 10^{-4}$	3,580	1.7 mA *
$1.0 \times 10^{-4}$	3,600	450 $\mu$ A
$5.0 \times 10^{-5}$	3,600	250 $\mu$ A
$1.0 \times 10^{-5}$	3,600	120 $\mu$ A
$5.0 \times 10^{-9}$	3,525	140 $\mu$ A

\*Starting Pulse (all other currents some seconds after start)

In taking the above data the variable inlet leak is opened to raise the system pressure to the value  $P_1$  with the ion pump off. As soon as the ion pump is started the pressure begins to drop and the time required to pump down to an equilibrium pressure is less than one minute, even with a starting pressure of  $1 \times 10^{-3}$  torr. A test was also conducted to determine the ion pump current and voltage at a given pressure by varying the leak rate with the pump on, until a stable pressure was attained at the required level. The results of this test are shown in Table 6.\*\*

TABLE 6.- CURRENT-VOLTAGE VERSUS PRESSURE

$P_1$ (torr)	$P_2$ (torr)	$I_p$	$V_p$ (Volts)
$5.0 \times 10^{-4}$	$7.2 \times 10^{-4}$	11.0 mA	2,850
$1.0 \times 10^{-4}$	$1.7 \times 10^{-4}$	2.8 $\mu$ A	3,300
$5.0 \times 10^{-5}$	$1.0 \times 10^{-4}$	1.7 $\mu$ A	3,400
$1.0 \times 10^{-5}$	$1.8 \times 10^{-5}$	370 $\mu$ A	3,580
$5.0 \times 10^{-6}$	$1.0 \times 10^{-5}$	244 $\mu$ A	3,600
$1.0 \times 10^{-6}$	$1.3 \times 10^{-6}$	105 $\mu$ A	3,620

\*\*This data was taken utilizing a Varian Associates Model 921-0015 Ion Pump Control Unit.



Having shown above that the ion pump can be started and operated at a greater pressure range than required, tests to measure the pumping speed were initiated.

The pumping speed of this ion pump fluctuated significantly from measurement to measurement, but was consistently low, ranging from about one liter per second to two and one-half liters per second at a pressure of  $1 \times 10^{-6}$  torr, even with an anode voltage of 5,000 volts. This pumping speed was, at best, somewhat over half the value expected. An intense investigation was therefore initiated to determine the cause for the low speed measured. The voltage was varied to determine the effect of voltage on pumping speed, since Varian design engineers had previously stated that voltage played a large part in determining the pumping speed for a given pump. The large variations were attributed to the low pumping speed combined with experimental variations.

Test results showed a dependence of pumping speed on voltage, as indicated in Figure 8, but it was not the strong dependence that was expected. In fact, the variations of pumping speed with anode voltage was not much greater than the repeatability variations from run-to-run. It was concluded that the geometry of the pump and the fields did not allow the pumping speed goal to be achieved, and an analysis of the discharge, including magnetic fields, was initiated. A consultant was also employed to take full advantage of existing knowledge, but no major causes could be identified. From the discharge analysis it was felt that the nonuniformity and the geometry of the magnetic field as well as its strength was more important than voltage. It was theorized that the field asymmetries combined with the physical pump geometry causes the discharge to change modes frequently due to instabilities and also it appears that discharges were formed outside of the anodes between the two anode cells. This leads to very ineffective pumping because most of the electrons produced are lost before they have a chance to ionize an appreciable number of gas molecules. This would be especially true at low pressures where molecules are fewer in number. This effect presents itself as a large ionization inefficiency or as an exceptionally large current at any given pressure, especially low pressures. Such an effect should be very obvious when the I/p parameter is examined. Reviewing Figure 8, note that at low pressures I/p is very high for the pumping speed. A normal diode pump should have an I/p from fifteen to forty amperes per torr per liters per second. When the I/p value runs into hundreds of amperes per torr per liters per second, it becomes apparent that very large instabilities of the discharge are occurring constantly. Analysis of the data indicated that because of the relatively small change in pumping speed with voltage, the pump must have been operating in the region where according to published data a change of magnetic field has a large affect on the pumping speed (see Figure 9).<sup>2</sup> To test

---

<sup>2</sup> Important Characteristics of New Type Getter-Ion Pump by R.L. Jepsen, 1959, Varian Associates, VR-7.

this hypothesis and to determine the effect of both field geometry and field strength several tests were run with various magnet configurations. The first specialized test was to run a single anode, by applying a magnetic field to only one anode, with a typical two liter per second Varian magnet and determine its approximate speed. This test provides one anode with the normal field geometry of a two liter per second Varian pump. Both left and right anode cells were tested in this manner with the test results shown in Figure 10. In all test data taken, the pumping speed in the  $10^{-5}$  torr region is disregarded because of pressure gauge uncertainties. Plots of the magnetic fields are shown in Figure 11. With the single cell test, the magnetic field, although weaker is much more uniform, therefore, the pumping speed may be considered to be about one and one-half liters per second for each cell under good field geometry and strength.

Field geometry and strength play a large role in determining the pumping speed because, as was shown in Equation (8), the field strength is inversely proportional to the radius of the electron orbits about a magnetic line. Since the electrons will generally spiral about the magnetic lines, the orientation of these lines is very important. These lines must be parallel to the anode surface and should not cross the anode walls. Any crossing of the walls by these lines will cause electrons spiraling around such lines to impact the anode walls and be eliminated. Elimination of such electrons, in turn, reduces the ionization rate of the gas molecules and also affects the discharge geometry, making it inefficient for pumping.

Two-two liter per second pump magnets were placed together to approximate a more uniform field distribution (see Figure 11) and tests were conducted with the results shown in Figure 10. The data was taken at 5,000 volts and no direct comparison could be made with the other configurations shown in Figure 10, which were taken at 4,000 volts. These experiments were repeated under more tightly controlled conditions and data was taken in both directions of pressure change; increasing and decreasing. The data is shown in Figures 12 and 13. On the surface, all the above data indicated that the low pumping speed could not be improved except by running the pump at higher voltages, as shown in Figure 14. The pumping speed in the desired pressure range however ( $10^{-6}$  torr), was not sufficient, even with 5,000 volts, and the electrical feedthrough on the pump could not be run over 5,500 volts.

The problem seemed to be the pump and field geometry. Figure 15 shows the desired magnetic field geometry versus the actual geometry. In order to approximate the desired geometry, the two-two liter per second Varian magnets were again placed together with a separation of about three-eighths inch between them, with the resulting magnetic field shown in Figures 16 and 17.

These two figures show that the field is very uniform at the anodes, but it is lower than the required field as defined in Figure 9. Several runs were made with the new configuration and the standard magnet. The data from these runs was compared as shown in Figure 18. This data indicates that some improvement has been achieved by the new configuration but it required a stronger magnetic field, which must be more adequately tested. Since a stronger magnet was not readily available, it was decided to consider other areas first. A test of the ion pump for argon pumping speed was conducted. The pumping speed with pure argon was exceptionally high and less variant than with nitrogen. It appears that the pumping speed for pure argon is about forty percent of that for nitrogen (see Figure 19). The pumping speed for argon was measured with the standard magnet (P-E magnet) designed for this pump.

When argon is used as the pumped gas in a diode type ion pump all the pump surfaces are either cleaned of buried impurities by the sputtering caused by the argon ions, or are covered by pure titanium or tantalum layers, since the argon cannot form a chemical compound with these two materials. The surface cleaning effect of argon can either be achieved by a long duration of running argon at low pressures or by a relatively short duration at high pressure. A clean titanium or tantalum surface will of course increase the pumping speed of a pump temporarily for active gases. This is due to active gas molecules colliding with the exposed (clean) titanium or tantalum layers and forming stable compounds thus in effect causing surface pumping until the exposed titanium on the surface is depleted.

The pumping speed for nitrogen was measured after the argon activation. The results for both increasing and decreasing pressures are shown in Figure 20. The data in this figure indicates that insufficient stabilization time was allowed before the data was taken, thus, the correct speed would be the average of both directions, or about two and one-half liters per second. Argon activation proved that the ion pump could pump argon stably and as expected, it increased the pumping speed of active gases for a temporary period after argon activation. While the argon test was being conducted, another temporary magnet was constructed similar to the standard P-E design (Figure 6). The two similar magnets were placed together with a spacing of approximately one-half inch and in a manner similar to the two-two liters per second magnet previously mentioned. The magnetic field strength was about one and one-tenth kilogauss, but the magnetic field was almost uniform in all directions in the vicinity of the anode cells. Several runs were made to test the affect of geometry and field strength and the results are shown in Figure 21. Observe that the uniformity of the field provides a greater change in pumping speed than a twenty percent increase in field strength. Figure 22 shows the affect of field strength variation on pumping

speed, Figure 23 shows the effect of geometry while Figure 24 shows the effect of voltage. The above figures immediately indicate that the magnetic field parameters are the most important, but that a much stronger uniform field, perhaps about 1,500 gauss is required to reach a speed of three liters per second with the present pump geometry. Such a field strength cannot be obtained over the total discharge area with a magnet having a reasonable weight. It was concluded that it would be necessary to change the geometry of the pump.

### Eight Cell Prototype

The pump geometry was reviewed, but it became immediately apparent that there was not complete freedom to redesign the entire ion pump. The restrictions resulted from the requirement that the ion pump developed on this contract was to be applied on the mass spectrometer system being developed for NASA Manned Spacecraft Center under contract NAS 9-9799. The pump housings for that contract were already designed and in fabrication and were based upon the initial two cell design. Any redesign therefore had to utilize these housings if at all possible.

The most obvious geometry change was to design the anodes so that they are immersed in a more uniform magnetic field. This manifests itself as a smaller anode diameter to reduce the field gradient within each anode. However, the anode diameter cannot be decreased arbitrarily, since the pumping speed is proportional to the product of the magnetic field strength and anode radius. Earlier experimental data (see NAS1-6387) has shown that in order for an ion pump to work efficiently at pressures of  $10^{-7}$  to  $10^{-5}$  torr, the minimum  $Br_a$  product must be greater than 400 gauss per centimeter. There was limited freedom to change the magnetic field strength and therefore a minimum anode radius was established. After analysis of the parameters it was determined that the optimum anode geometry was an anode assembly composed of eight cells. Each of the cells would be one-half inch in diameter. With an average field strength of one kilogauss the  $Br_a$  product is then approximately one and three-tenths kilogauss per centimeter, well above the minimum. The eight-cell anode configuration also increased the usable cathode area from about one square inch to over one and one-half square inches. The anode length was reduced from about one inch to about 0.87 inch, which only decreased the discharge volume slightly. It was found in the literature<sup>2</sup> that a single cell of five-tenths by nine-tenths of an inch could provide a pumping speed of up to one liter per second (see Figure 9). With the magnetic field strength available and an operating voltage of about 4,000 volts,

---

<sup>2</sup> Refer to footnote on Page 14

it was felt that the eight cells would provide a pumping speed of between three and four liters per second. All the analyses pointed towards success of the eight-cell configuration. But as an added precaution, the magnet was redesigned to increase the magnetic material and the pump housing over the cathodes was made of magnetic material in order to provide a more uniform magnetic field. Figures 25 and 26 show the final configuration of the Eight-Cell Prototype Ion Pump. The tantalum posts were eliminated because experimental or theoretical data, which would substantiate their value is not available, and it would be more difficult to locate the posts in an eight-cell design with smaller cathodes. The Eight-Cell Prototype Ion Pump was fabricated with the intent of proving the new geometry of the anode and magnetic pole faces. No effort was expended to design a noble gas pumping capability in the prototype, therefore, two titanium cathodes were utilized.

The prototype pump was tested with a typical pumping speed versus pressure characteristic as shown in Figure 27. Pumping speed, as a function of voltage at a constant pressure of  $1$  to  $2 \times 10^{-6}$  torr, is shown in Figure 28. From this figure note that the pumping speed levels off above 4,000 volts. This indicates that the magnetic field is not at an optimum strength for the intended operating anode voltage. With a field strength of about 1,500 gauss, the pumping speed could possibly be over six liters per second. The present pumping speed of about four liters per second is adequate however, so no attempt was made to change the magnet geometry. The prototype pump was tested for argon pumping and as expected it would not pump argon after the cathodes were argon saturated.

A pumping speed test was also conducted with air as the sample gas. The pump went into argon instabilities after a period of time as would be expected. The ion pump design used in the prototype can easily be changed to an argon stable pump by merely changing one of the cathodes from titanium to tantalum. A titanium/tantalum pump can pump argon at about twenty-five percent of the pumping speed of nitrogen.

The redesigned prototype was tested for starting characteristics including starts and runs with the newly designed breadboard power supply\*. Figure 29 shows the voltage required to start the ion pump at a given pressure in the high pressure region. The pump was successfully started at pressures between  $10^{-9}$  and  $10^{-3}$  torr.

---

\*See Volume 3 of 6 of this final report.

The prototype was also tested for pumping speed variations versus time at a pressure of approximately  $2 \times 10^{-6}$  torr for over sixteen days (see Table 7). The test gas at first was air, but argon in the air caused the pump to exhibit instabilities. The air sample was replaced by nitrogen and the test continued. The test showed no time effect on the pumping speed other than the normal experimental variations.

TABLE 7.- LONG TERM ION PUMP TEST

Days	$P_1$ (torr)	$P_2$ (torr)	$E_p$ (volts)	$I_p$ ( $\mu$ A)	$S_p$ ( $\ell$ /sec)	Gas
1	$2.0 \times 10^{-6}$	$7.6 \times 10^{-6}$	3,950	225	4.5	Air
2	$1.7 \times 10^{-6}$	$6.8 \times 10^{-6}$	4,000	180	4.9	Air
PUMP OPERATION WITH ARGON INSTABILITIES BECAUSE OF ARGON IN AIR. CHANGED PUMPED GAS TO $N_2$ .						
2	$2.4 \times 10^{-6}$	$7.8 \times 10^{-6}$	3,780	300	3.64	$N_2$
3	2.4	7.7	3,770	310	3.56	
4	2.4	7.6	3,750	320	3.5	
5	1.9	6.1	3,880	250	3.56	
6	1.8	5.8	3,900	240	3.6	
9	1.6	5.0	3,960	200	3.4	
10	2.2	6.8	3,780	300	3.4	
11	2.2	6.7	3,790	295	3.3	
12	2.2	6.7	3,770	300	3.3	
15	1.8	5.7	3,940	250	3.2	
15	2.1	7.6	4,800*	280	4.2	
15	2.0	6.9	>4,000**	290	3.9	
16	2.0	7.0	>4,000	300	4.0	

\*Changed to lab power supply    \*\*Changed to flight breadboard power supply

As noted in Table 7, the flight breadboard power supply was allowed to run the pump as part of the long duration test. This power supply has two modes of operation, first, the high voltage mode is at 4,800 volts and second, the low voltage mode is at 800 volts. The power supply stays in the high voltage mode until the pump draws approximately one milliampere of current, at which time it switches to the low mode, which can draw up to twelve milliamperes. It stays in the low voltage mode until the current demand is less than 100 microamperes, at which time it switches back to the high mode. The pressure levels at which the switching occurs are shown in Table 8.

TABLE 8.- PUMP POWER SUPPLY BEHAVIOR

$P_1$	$P_2$	$I_p$	$E_p$	Mode	Comments
$2.0 \times 10^{-8}$	$4.8 \times 10^{-8}$	$< 5 \mu A$	4,800	High	Background increased inlet leak
$2.0 \times 10^{-7}$	$6.5 \times 10^{-7}$	20 $\mu A$	4,800	High	
$6.25 \times 10^{-7}$	$2.15 \times 10^{-6}$	60	4,800	High	
$1.0 \times 10^{-6}$	$3.7 \times 10^{-6}$	120	4,800	High	
$6.2 \times 10^{-6}$	$2.0 \times 10^{-5}$	820	4,800	High	
$7.2 \times 10^{-6}$		960			Switched to low mode Reduced inlet leak
$7.5 \times 10^{-6}$	$8.6 \times 10^{-6}$	205	800		
$7.0 \times 10^{-6}$	$7.6 \times 10^{-6}$	190	800		
$3.4 \times 10^{-6}$		100			Switched to high mode
$2.2 \times 10^{-7}$	$5.6 \times 10^{-7}$	25	4,800		

## ROUGH PUMPING

When the mass spectrometer system is vented, provisions must be made to rough pump the system down, from the resulting high pressure, to at or below the ion pump starting pressure of at least  $10^{-2}$  to  $10^{-3}$  torr, so that the ion pump can be started.

There are several methods which may be utilized for rough pumping, but they all must be useful in a spacecraft environment. The following are methods considered in this report.

- a. Vacuum line to outer space
- b. Cryo-sorption pumping
- c. Sublimation pumping

#### Vacuum Line to Space

If the mass spectrometer system is vented to some high pressure the system can be pumped down to or below the ion pump operating pressure by using a line to outer space. This line is connected between the mass spectrometer system and the outside surface of the vehicle. A valve, or some type of breakaway hat must be provided to maintain the vacuum in the system while the spacecraft is at the launch condition. A valve inside the spacecraft is probably more desirable for easy access, but allows part of the line (outside of the valve) to be contaminated with atmosphere. This in turn will slow the pumpdown time when the valve is open, but is overshadowed by the ease of access and safety considerations in the event of a large leak in the mass spectrometer.

In order to establish the feasibility of a roughing vacuum line a computation was made to determine the line diameter required to achieve a pressure suitable for ion pump starting in a fixed time. The following assumptions and parameters were employed:

- a. Molecular flow in line (constant conductance).
- b. The volume of the system to be pumped is one liter.
- c. Initial system pressure is one atmosphere.
- d. Pressure required for starting the ion pump is  $10^{-4}$  torr.
- e. Pumpdown time required is 100 seconds.

The differential equation for evaluation of a volume through a fixed conductance vent, in the pressure of an inflow of gas through a leak from a higher pressure source, is:

$$V \frac{dP}{dt} = (P_s - P) C_o - (P - P_o) C \quad (13)$$



where  $V$  = Volume to be pumped out  
 $C_o$  = Leak into the system  
 $P_s$  = High pressure side of  $C_o$   
 $P$  = Pressure of system  
 $P_o$  = Ultimate pressure of space  
 $C$  = Conductance of pump out line

rearranging the terms of Equation (13)

$$\begin{aligned} \frac{dp}{dt} &= P_o \frac{C_o}{V} + P_s \frac{C}{V} - P \left( \frac{C_o}{V} + \frac{C}{V} \right) \\ &= \frac{P_o}{\tau_s} + \frac{P_s}{\tau} - P \left( \frac{1}{\tau_s} + \frac{1}{\tau} \right) \end{aligned} \quad (14)$$

In normal operation the leak into the mass spectrometer would be shut-off when pumping out to space, thus  $C_o = 0$ . Equation (14) would then become:

$$\frac{dp}{dt} = - \frac{P}{\tau} + \frac{P_o}{\tau} \quad (15)$$

which gives upon integration

$$P_f = P_o + (P_i - P_o) e^{-t/\tau}$$

where  $P_f$  = Final pressure required ( $1 \times 10^{-4}$  torr)

$P_i$  = Initial pressure (760 torr)

$P_o$  = Ultimate space vacuum

$\tau$  = Time constant

$t$  = Required pumpdown time (100 sec)

for  $P_i > P_f \gg P_o$

$$P_f = P_o + P_i e^{-t/\tau}$$

$$\frac{P_f}{P_i} = e^{-t/\tau}$$

$$\begin{aligned}\tau &= t / \ln \left( \frac{P_i}{P_f} \right) = 100 / \ln (7.6 \times 10^6) \\ &= 6.3117 \text{ sec}\end{aligned}$$

This time constant requires a line conductance of

$$C = \frac{V}{\tau} = \frac{1}{6.3} = 0.158 \text{ l/sec}$$

Since for molecular flow:

$$C = 12.1 \frac{D^3}{L}$$

where  $D$  = Diameter of line (cm)

$L$  = Length of line (cm) = 300

$$D^3 = \frac{(0.158) (300)}{12.1}$$

$$D \approx 1.5 \text{ cm or } 0.59 \text{ inch}$$

This diameter is feasible in terms of typical spacecraft interface requirements.

#### Cryo-Sorption Pumping

A very clean method of roughing down a vacuum system is by use of sorption pumps which utilize a sorptive material such as a Molecular Sieve to trap the gases. Unfortunately, however, these pumps require cryogenic temperatures for efficient operation. To attain these low temperatures in the laboratory, liquid nitrogen is used. However, liquid nitrogen cannot be used in a spacecraft application since it is not available in the spacecraft. The alternative to using cryogenic liquids is to operate at least two pumps in a cascade fashion at room temperature (baking them and cooling them to room temperature) or to use thermoelectric cooling.

The technique of cascading two pumps at room temperature was tested in the laboratory to determine the minimum pressure which can be obtained by this method. Figure 31 shows the test setup, while Table 9 shows the test data. The lowest pressure obtained using this method, as noted from Table 9, was 34 torr. With a fresh molecular sieve the pressure could probably be reduced to about one torr by cascading two pumps at room temperature. Even at one torr, however, the pressure is still at least two orders of magnitude above the pressure at which an ion pump can be efficiently started and operated. In order to further decrease the pressure by use of sorption pumps, the temperature of the pump has to be decreased.

Since cryogenic liquids are not conveniently available for this use in a spacecraft, using thermoelectric cooling to achieve lower temperatures is possible. Thermoelectric cooling can provide a maximum temperature difference of seventy degrees centigrade between the hot and cold junctions. If the hot junction is maintained at a room temperature of twenty-five degrees centigrade by use of a heat sink, then the minimum temperature attained at the pump can be as low as minus forty-five degrees centigrade. At this temperature a cryo-sorption pump can reduce the pressure at least another one and a half decades below that at room temperature or about one torr with the test pumps mentioned above.

Several experiments were conducted to obtain the minimum pressures attainable at zero, minus eighty and minus 195 degrees centigrade. The data for zero and minus eighty degrees centigrade are shown in Tables 10 and 11 respectively. The minimum pressures attained are plotted in Figure 32. These points appear to be about one to three decades higher than the theoretical value (see Figure 33). For this reason a test was run with liquid nitrogen, which will allow a pump to reach at least  $10^{-5}$  torr with air as the pumped gas. The pressure achieved with this method was about fifteen microns or  $1.5 \times 10^{-2}$  torr. This check point, which is above the theoretical value by up to three decades, indicates that the pumps required longer rejuvenation (bakeout) or replacement of their sieve. The correction of up to three decades cannot be arbitrarily made at temperatures above minus 100 degrees centigrade. This is due to the efficiency of pumping of different gases. For example, at room temperature and down to zero degrees centigrade no argon pumping will occur. Thus, if air is the pumped gas the pressure cannot be decreased below approximately eight torr, which is the partial pressure of argon in the atmosphere.

Figure 34 shows the relative pumping efficiency for argon, nitrogen and oxygen versus temperature below zero degrees, for a typical zeolite. Using this figure, note that if a thermoelectric cooling of minus forty-five degrees centigrade is utilized a much lower pressure can be attained if the system is first purged with nitrogen, since the molecular sieve has a greater

TABLE 9.- CRYO-SORPTION PUMPING AT 25°C

Time	Pressure (torr)	Comments
1622	730	Open $P_1$ volume at 1 Atm
1623	468	Open $P_2$ both open
1625	288	Close $P_1$ to bake-out
1630 - 1800	283	$P_2$ Open; $P_1$ in bake-out
1800	283	Stop bake-out; close both pumps
0827	293	Open $P_1$ $P_2$ in bake-out
0830	95	Open $P_1$ $P_2$ in bake-out
1045	101	Close $P_1$ $P_2$ in bake-out
1055	102	Close $P_1$ end bake-out
1057	102	Open $P_1$ open $P_2$
1058	137	Open $P_1$ close $P_2$ to cool
1105	136	Close $P_1$ for bake-out $P_2$ closed
1205	137	Close $P_1$ for bake-out open $P_2$
1212	37	Close $P_1$ for bake-out open $P_2$
1415	34	Close $P_1$ for bake-out open $P_2$
1520	45	Open both pumps
1527	42	$P_1$ open $P_2$ closed

END OF TEST.-  $P_1$  PROBABLY NEEDS FRESH ZEOLITE.

TABLE 10.- CRYO-SORPTION PUMPING AT 0°C

Time	Pump	Temperature (°C)	Pressure (torr)	Comments
1305	#1	290	730	Bake-out off
1330	#1	130	730	Add H <sub>2</sub> O jacket
1335	#1	40	730	Add ice + H <sub>2</sub> O
1347	#1	7	730	Add ice + H
1359	Open #1	3	70	
1415	Open #1	0	51	
1623	Open #1	2	37	Close #1 Cool #2
1655	Open #2	~0	8	END TEST

TABLE 11.- CRYO-SORPTION PUMPING AT DRY-ICE TEMPERATURE

Time	Temperature (°F)	Pressure	Comments
1112	72	748 torr	Open #1 pump
1335	73	177 torr	Add CO <sub>2</sub> + methanol
1347	-90	33 torr	Add CO <sub>2</sub> + methanol
1308	-110	6 torr	Add CO <sub>2</sub> + methanol
1512	-110	3.7 torr	Open hot pump into cold pump (#1 + #2)
1730	-90	5.0 torr	Close #1 Cool #2 (open)
1731	-87	200 μ	Close #1 Cool #2 (open)
1815	-100	125 μ	Close #1 Cool #2 (open)
1955	-93	160 μ	END TEST

affinity for nitrogen at this temperature than for either oxygen or argon. With single stage thermoelectric cooling, cascading of two cryopumps and nitrogen purging of the system prior to pumpdown, reaching pressures of about  $10^{-3}$  torr is possible and is adequate for ion pump starts.

Single stage thermoelectric cooling can achieve a temperature difference, as mentioned above, of about seventy degrees centigrade but this is with no load on the system. The time and temperature differential of a given system can be calculated using the following formula:

$$Q = M C_p \frac{\Delta T}{\Delta t}$$

where  $Q$  = Heat removed (BTU/hr)

$M$  = Weight of material to be cooled (lbs)

$C_p$  = Average specific heat (BTU/lb - °F)

$\Delta t$  = Time required to cool (hr)

$\Delta T$  = Required temperature change (°F)

The actual operation of the system is dependent upon the geometry and heat losses, but cursory calculations show that within one hour a pump can be cooled to about minus twenty degrees centigrade with about thirty to forty watts. This will bring the pressure down to about  $10^{-3}$  torr in a nitrogen purged system as described above.

Thermoelectric cooling of sorption pumps, which are cascaded and nitrogen purged, is sufficient to pump a system from atmospheric pressure to a pressure low enough to start and operate an ion pump.

#### Sublimation Pumping

Another method for rough pumping that was considered is the use of sublimation of titanium. Titanium filaments can be heated to sublime titanium atoms, which then combine with nitrogen atoms to form Titanium Nitride (TiN) and stick to the surface of the pump housing.

Let the volume of the system to be pumped be equal to one liter. If the system is purged with nitrogen at atmospheric pressure there will be

$$\frac{6.023 \times 10^{23}}{22.4} = 2.78 \times 10^{22} \text{ molecules of } N_2$$

or  $5.56 \times 10^{22}$  atoms of N

Since the pressure required to start an ion pump is about  $10^{-3}$  torr, there are approximately  $7 \times 10^{16}$  atoms of nitrogen present. Thus, the number of atoms required to be pumped to reach that pressure is

$$5.5 \times 10^{22} - 7 \times 10^{16} \approx 5.5 \times 10^{22} \text{ atoms of N}$$

The largest commercial sublimation pumps can sublime titanium at about one gram per hour, which is about  $3 \times 10^{18}$  atoms per second. The rate required to successfully pump from one atmosphere of pressure is about 5,000 grams per hour. When this is compared to the power required for normal sublimation pumps, about fifty amperes at about three-tenths of a gram per hour, even if the current was linear with respect to rate of sublimation (which of course is not) it would take about one mega-ampere at about seven volts.

Of course, the above numbers are idealized for maximum speed or minimum time of pumpdown. By using realistic values of usable titanium and disregarding time it would still be unrealistic to use sublimation pumping to rough down the system. Let the usable titanium be one gram (most pumps of usable size), then the maximum gas load which can be pumped is

$$Q_{\max} = \frac{1 \text{ gm}}{(2)(48)} (22.4)(760) = 177.3 \text{ torr liters}$$

If the volume is one liter, then the pressure is reduced by 177 torr. At a normal current of about fifty amperes it would take about three hours for this reduction to occur.

## CONCLUSIONS

As a result of the above effort, a light weight and reliable ion pump has been constructed with a pumping speed that is compatible with the Two Gas Atmosphere Sensor Mass Spectrometer. A comparison of the flight pump with a commercial pump is given in Table 12 and indicated the substantial reductions which have been achieved in weight and size for a given pumping speed.

TABLE 12.- ION PUMP COMPARISON

Type	Speed (ℓ/sec)	Weight (lbs)	Volume (in <sup>3</sup> )	Voltage
Commercial	4-5	8.5	78	3,200
Flight Pump	3.6-4	3.3	24	3,800

With the understanding of ion pumps obtained as a result of this effort, improvements in pumping speed, weight and volume can be made with relatively little additional effort. The state-of-the-art advancement is believed to be attainable by reshaping the cathode surfaces and the magnetic fields. The required magnetic field can even be attained entirely or in part by anode assemblies which are magnetic.

A magnetic anode may reduce or completely eliminate the requirement of an external magnet. Any additional effort, however, should not be limited to improving diode type pumps. Triode configurations may prove to be useful in some applications, so they should at least be studied.

The analysis of the various rough pumping techniques indicates that the most efficient and reliable method of pumping a system is the use of a line to outer space. If this method is undesirable, because of the need to interface with the spacecraft skin, then the alternate acceptable method would be to use cryo-sorption pumps, cascaded at room temperature, to reach a pressure of approximately  $10^{-1}$  torr, then use a small sublimation pump to reduce the pressure from 100 microns to about  $10^{-4}$  torr or below the point at which the ion pump may be started with minimum current surge. Cryo-sorption pumps may also be cascaded in conjunction with thermoelectric cooling (if time allows) to directly reach a pressure of about  $10^{-3}$  torr, where the ion pump can be started and, thus, eliminate the use of a sublimation intermediary pumping system.



## APPENDIX A

## Magnet Design Criteria

To design the magnet for the ion pump the following criteria were utilized.

The length of the air gap ( $L_g$ ) is fixed by the geometry of the pump, which is one and one-half inches thick. The width of the magnet ( $W$ ) was fixed at two inches with its thickness ( $T$ ) fixed at one inch. These two dimensions were adequate to cover the two anodes within the pump where the field is required.

The above dimensions give a gap area ( $A_g$ ) of 2 and a

$$\frac{A_g}{L_g} = \frac{2}{1.5} = 1.33$$

knowing that

$$\frac{W}{T} = 2$$

By examining published graphs<sup>3</sup>, the ratio of pole strength  $B_p$  to center of gap strength  $B_g$  can be determined. This is found to be

$$\frac{B_p}{B_g} = 3$$

Having a requirement of 1,200 gauss for the field strength at the gap center, a pole strength of over 3,600 gauss is required. If the magnetic material is Alnico 9 then a slope ( $B/H$ ) of about 2.5 is required to supply the 3,600 gauss.

The length of the magnet may then be found by use of published graphs which give a magnet length of slightly over one inch. The magnet volume is then

$$2 (A_g)(L) = 2 (2)(1) = 4 \text{ in}^3$$

---

<sup>3</sup> G.E. Permanent Magnet Manual and Application Data

The density of Alnico 9 is about 0.262 pounds per inch cubed, which gives a magnet weight of 1.048 pound. The magnet yoke is Armco with about a 4.7 inch cubed volume. The density of the Armco is 0.298 pound per inch cubed, which makes the yoke about 1.4 pound. The total magnet weight is then about 2.5 pounds.

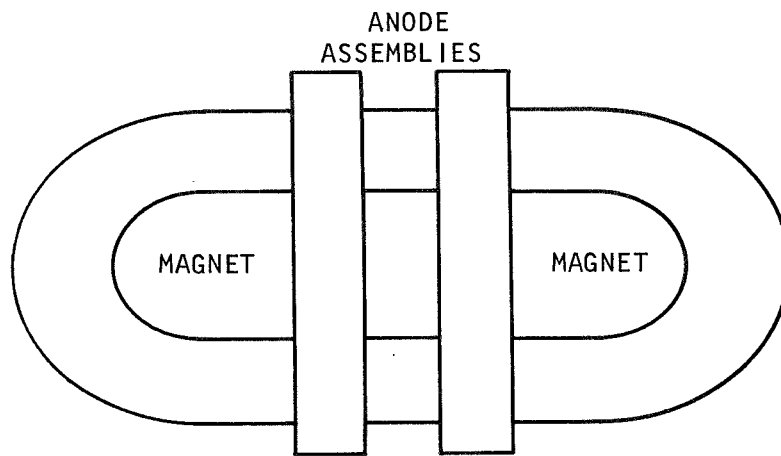


FIGURE 1.- Closed Ring Magnetic Circuit

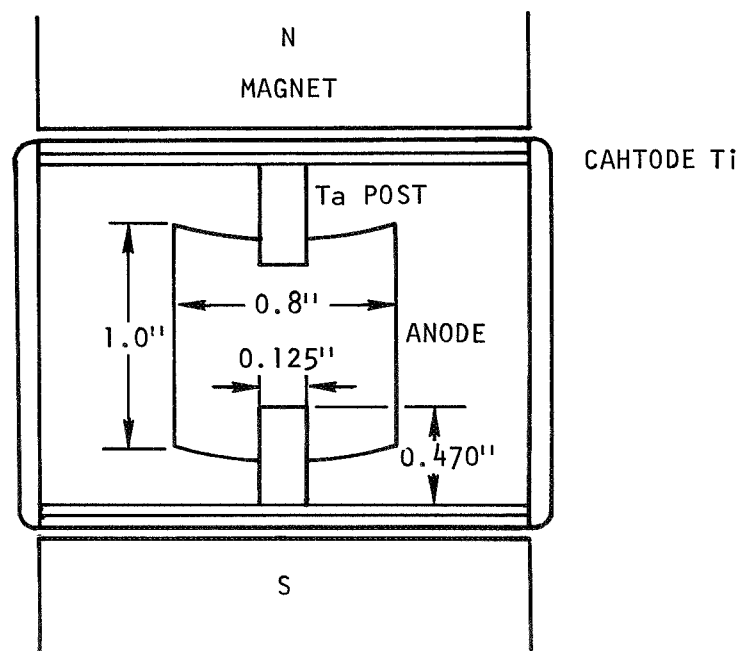
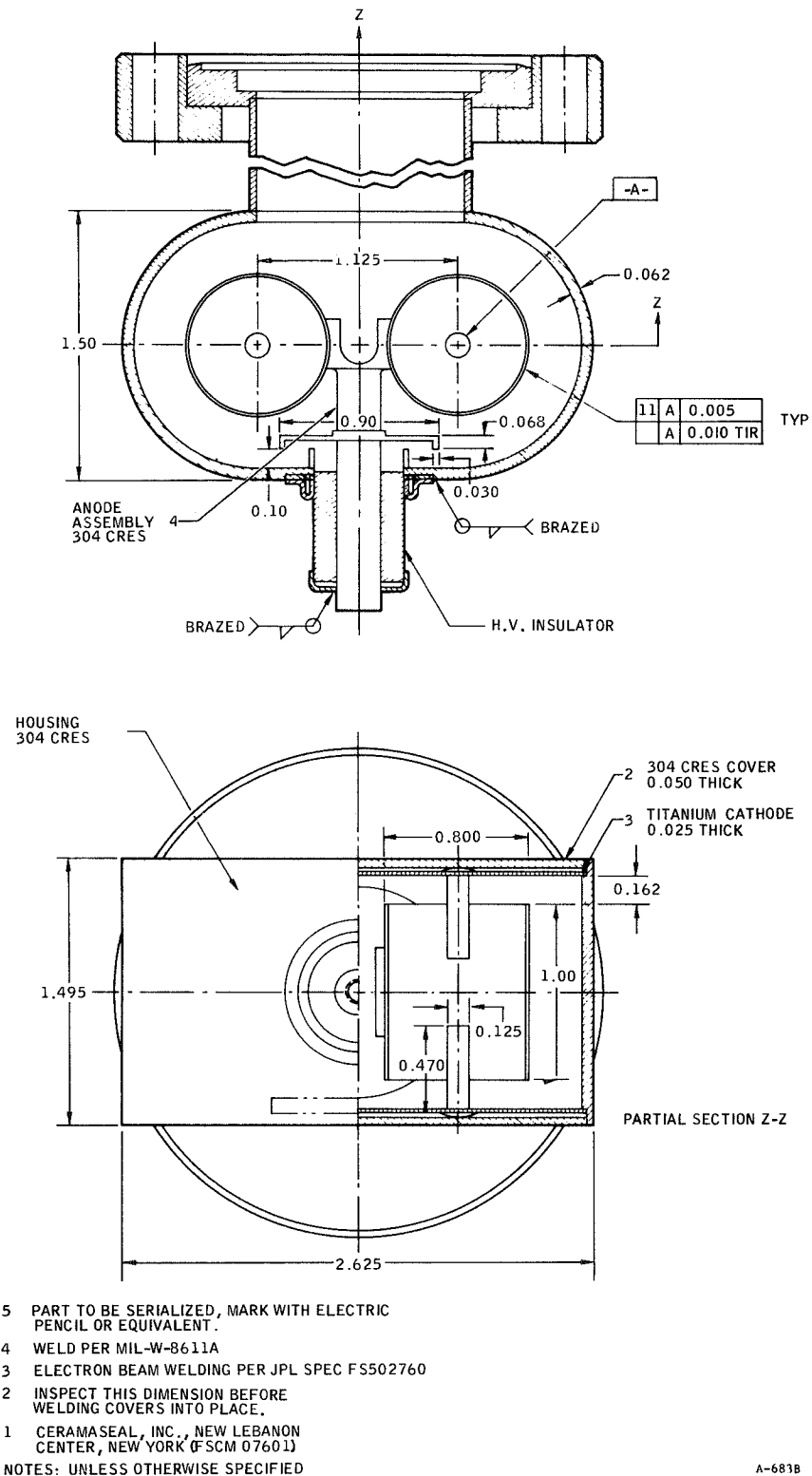


FIGURE 2.- Varian Two Liter per Second Ion Pump



A-683B

FIGURE 3.- Two-Cell Prototype Ion Pump

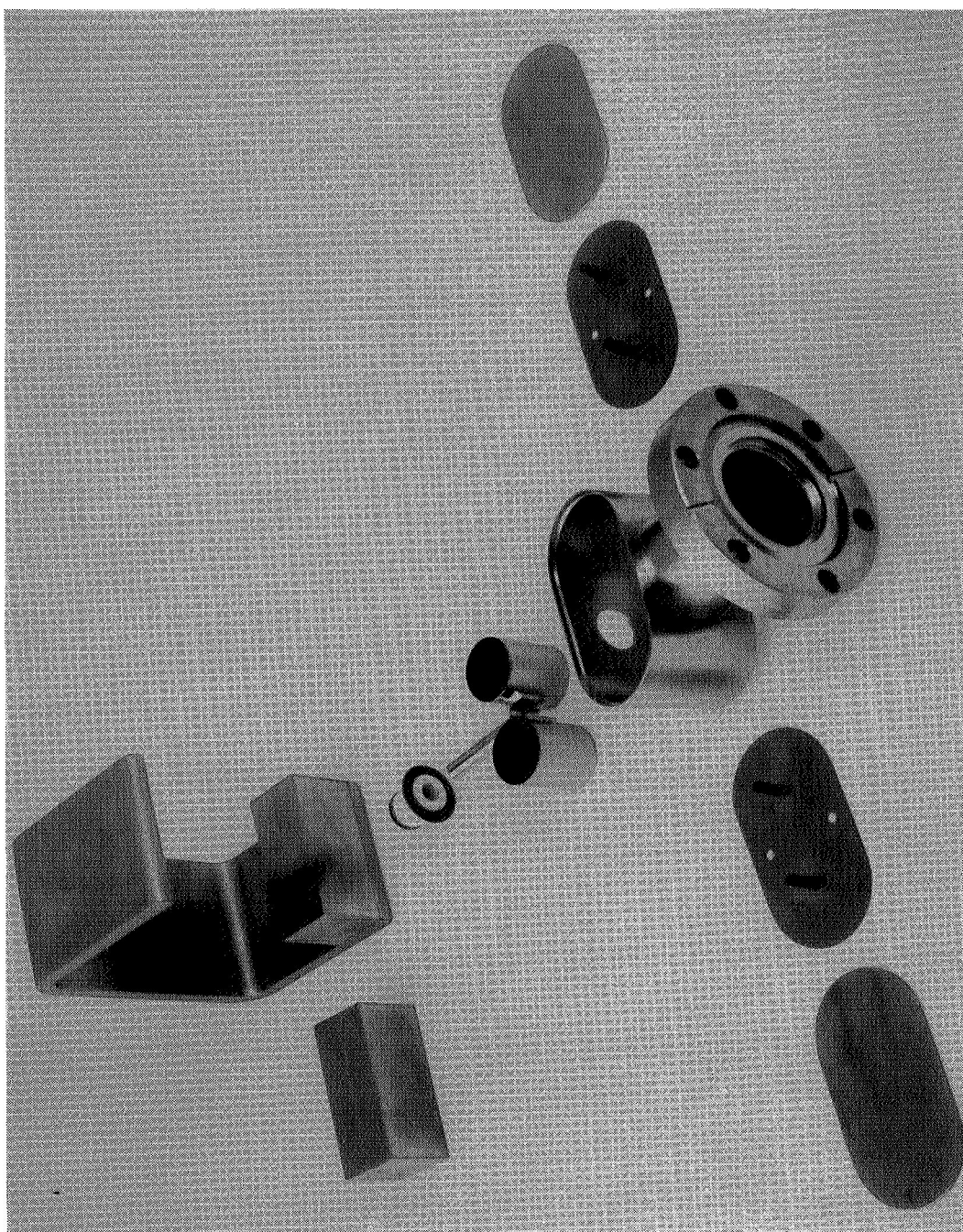


FIGURE 4.- Exploded View of Prototype Ion Pump

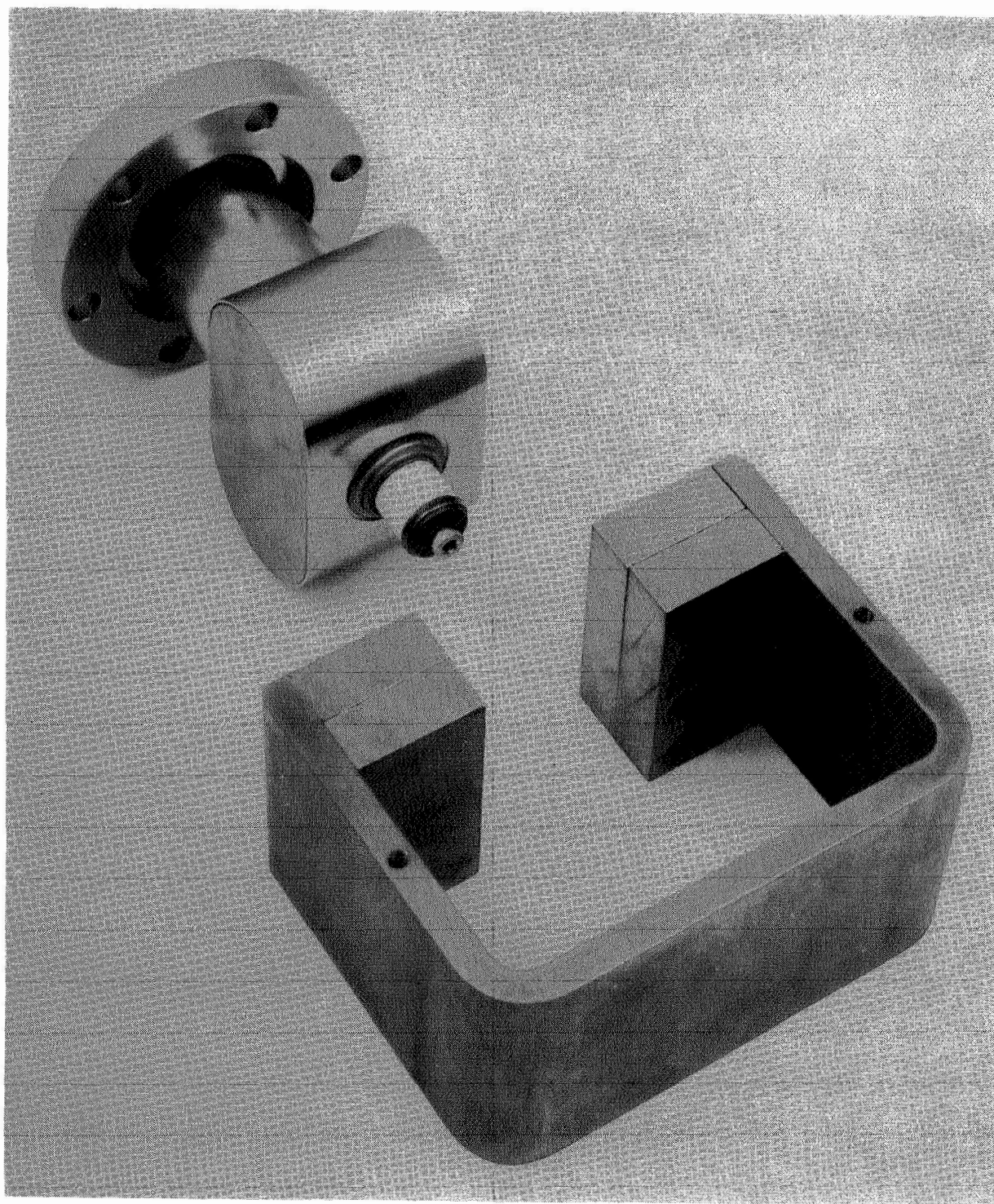


FIGURE 5.- Ion Pump Assembled (Prototype)

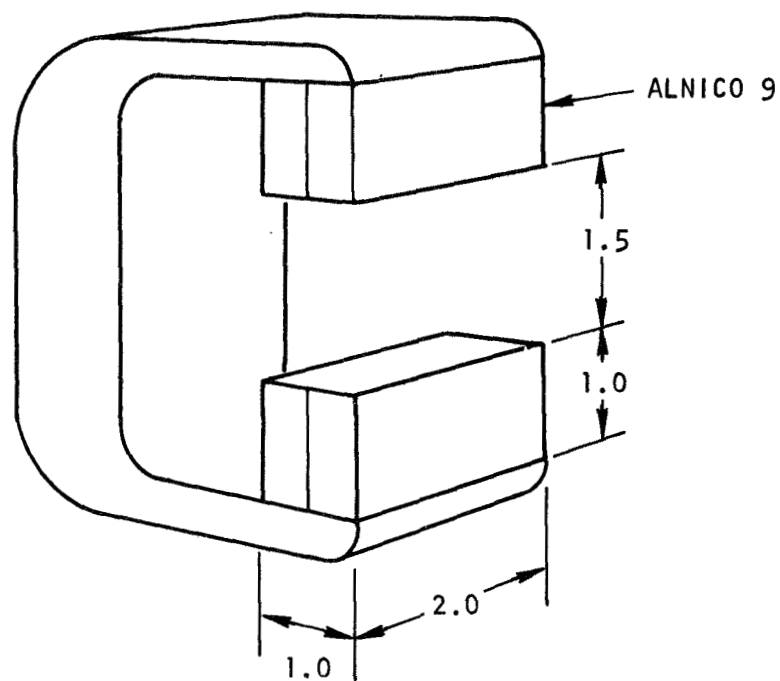


FIGURE 6.- Magnet Geometry

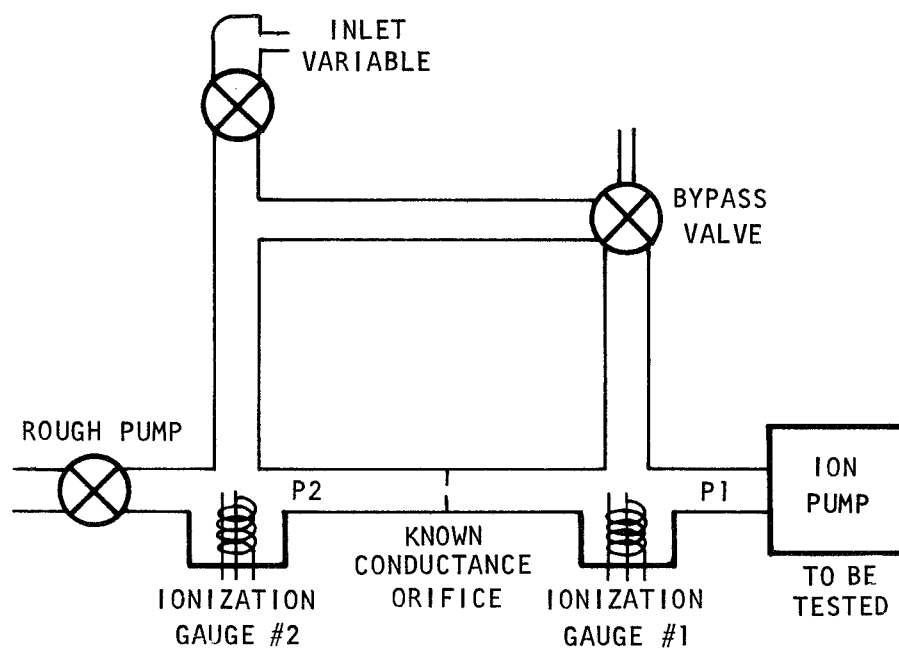
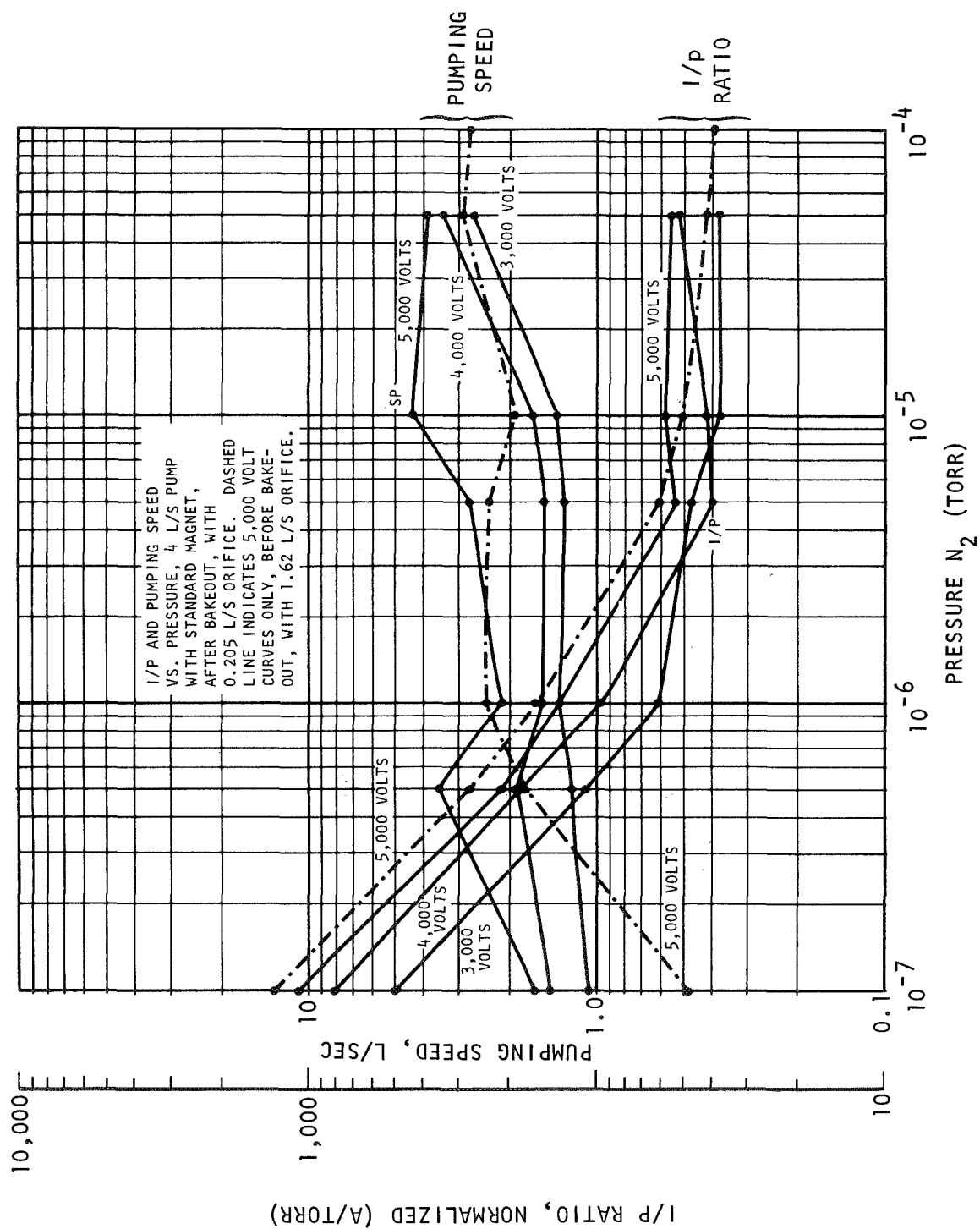


FIGURE 7.- Test Vacuum System





CATHODES OF TITANIUM  
 CATHODE SPACING  $\approx$  1.4 INCHES  
 ANODE LENGTH  $\approx$  0.9 INCHES  
 ANODE DIAMETER  $\approx$  0.5 INCHES  
 PRESSURE  $\approx$   $-5 \times 10^{-5}$  MILLIMETERS  
 OF MERCURY

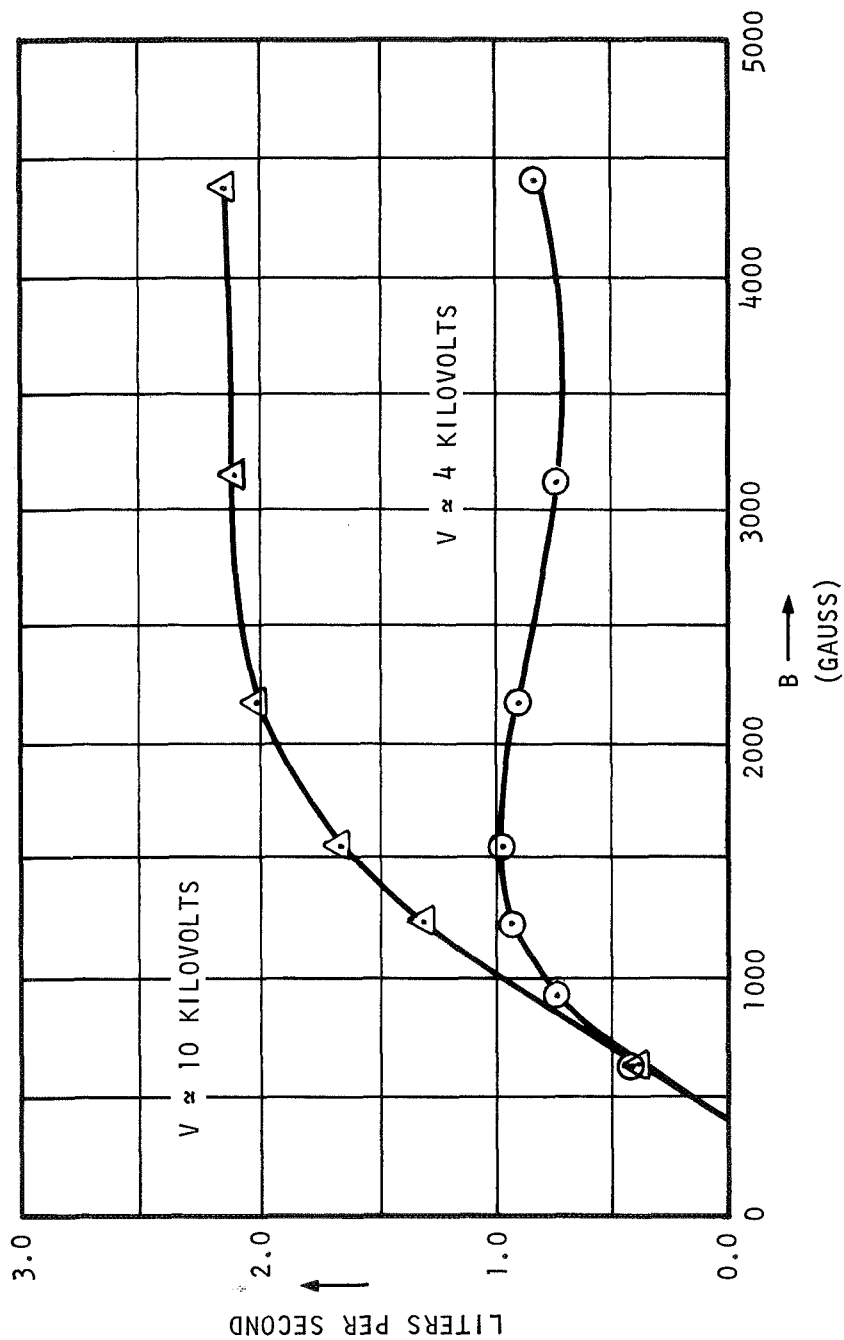


FIGURE 9.- Typical Variations of Speed (Single Cell) With Magnetic Field  
 for Two Values of Anode Voltage

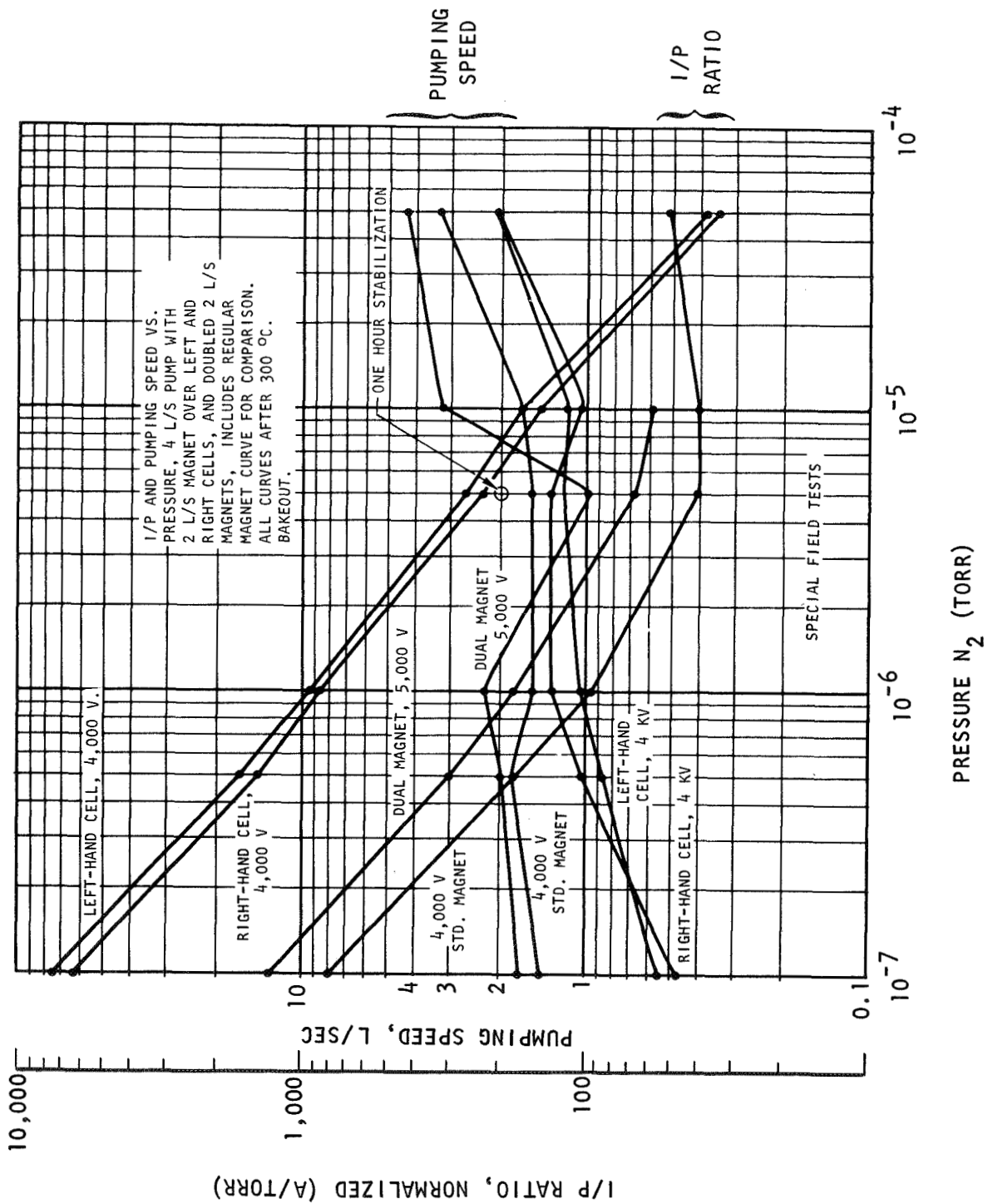


FIGURE 10.- Test Results

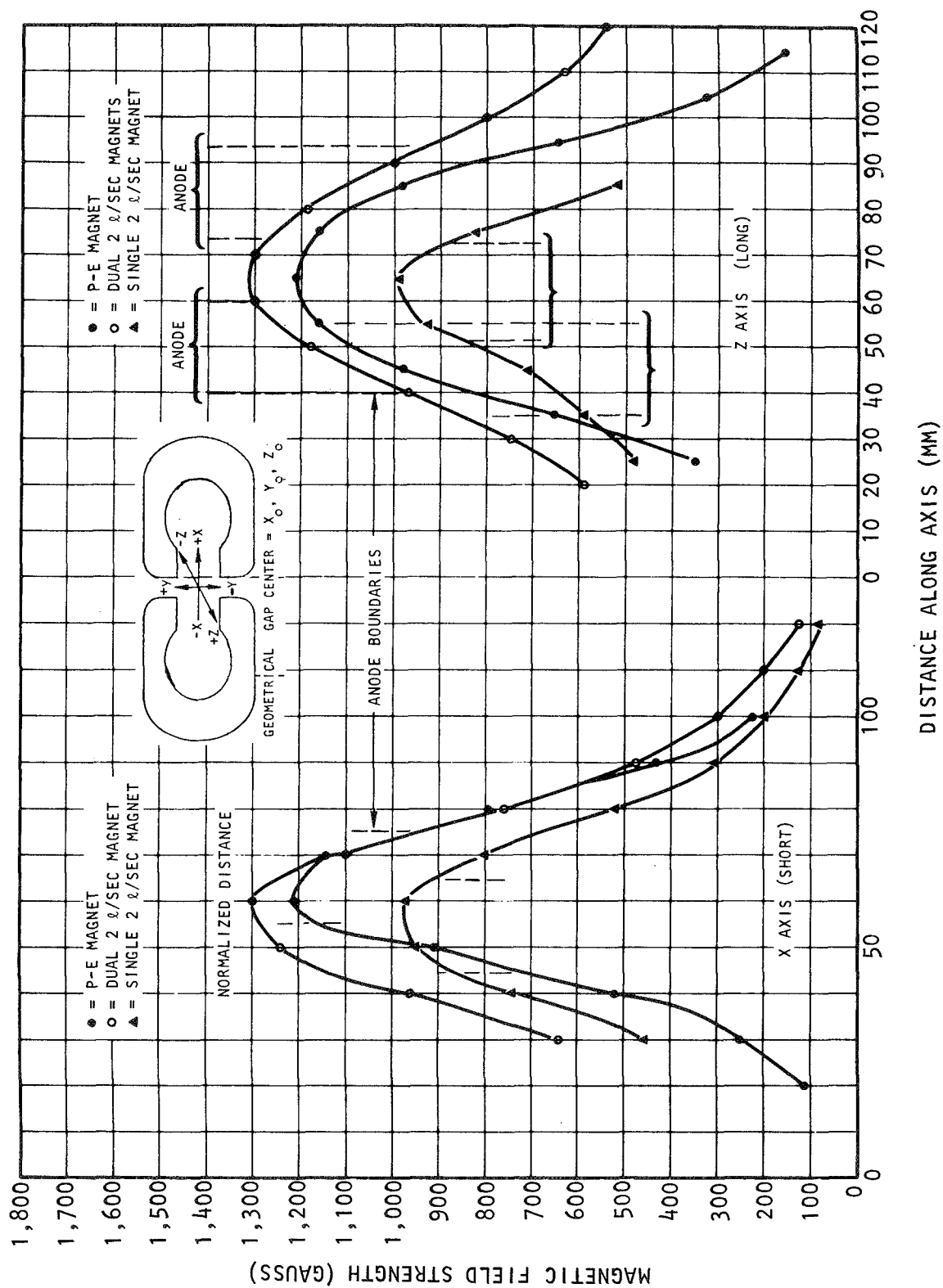


FIGURE 11.- Magnetic Field Plots

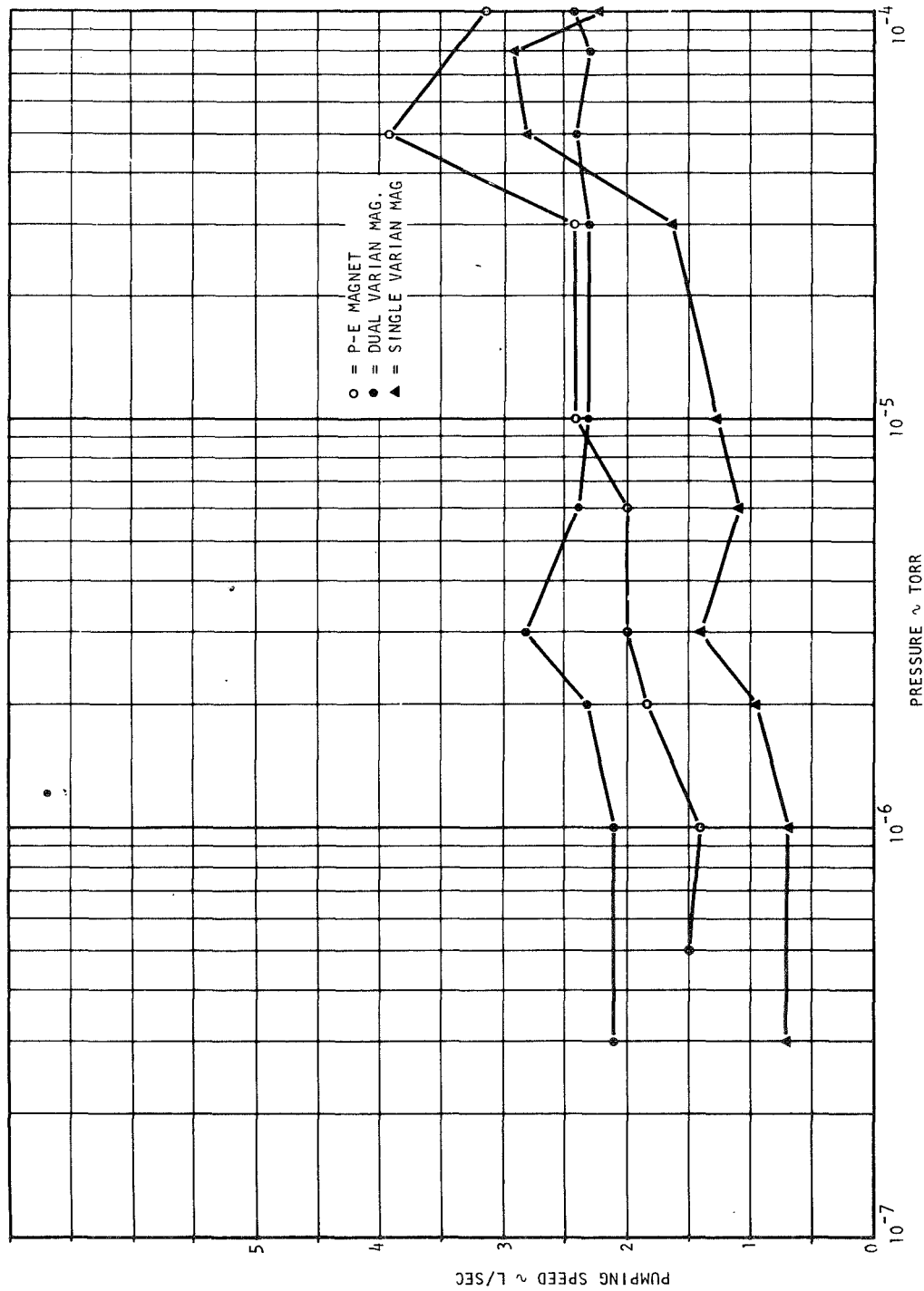


FIGURE 12.- Test Data Rerun

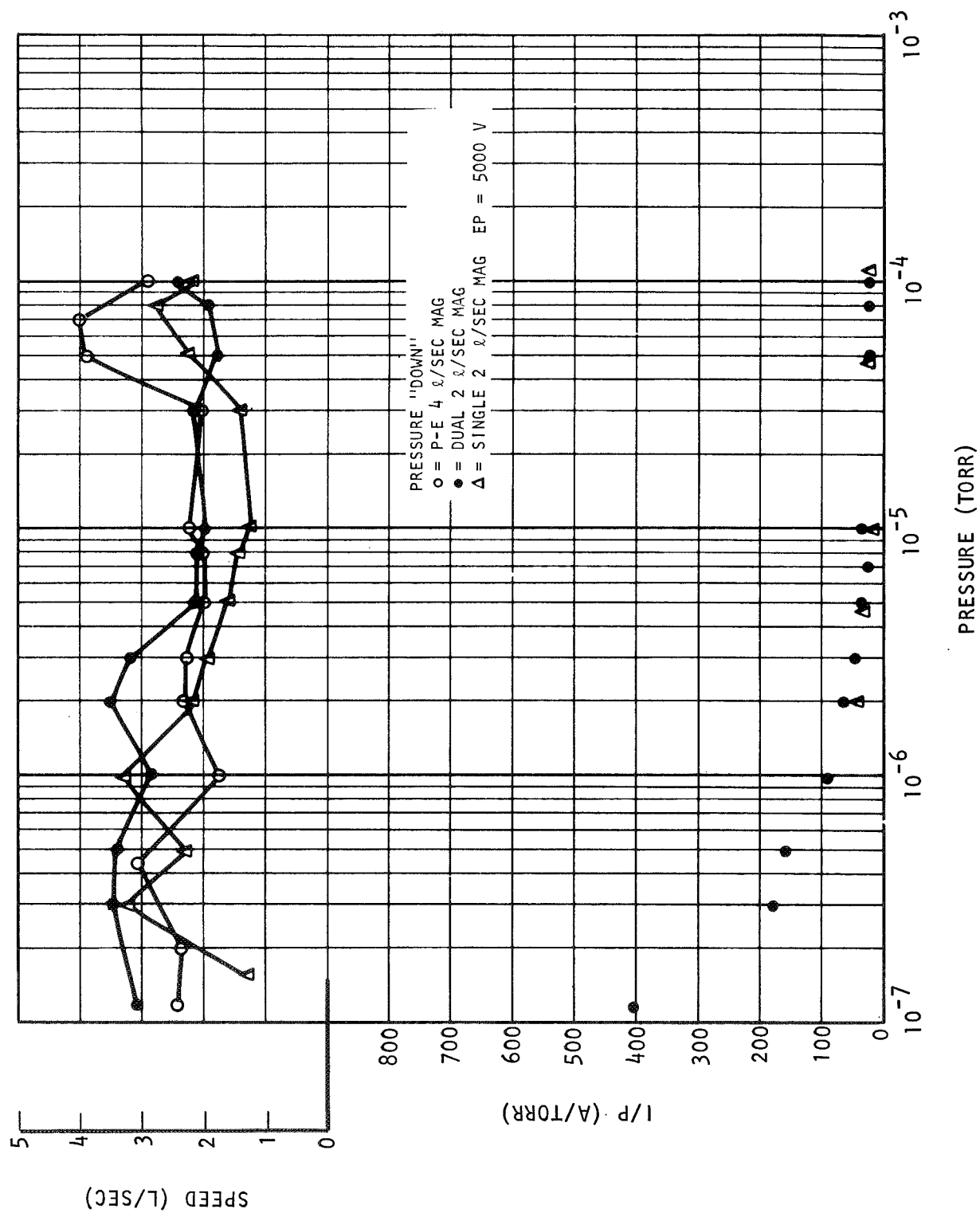


FIGURE 13.- Test Data Rerun

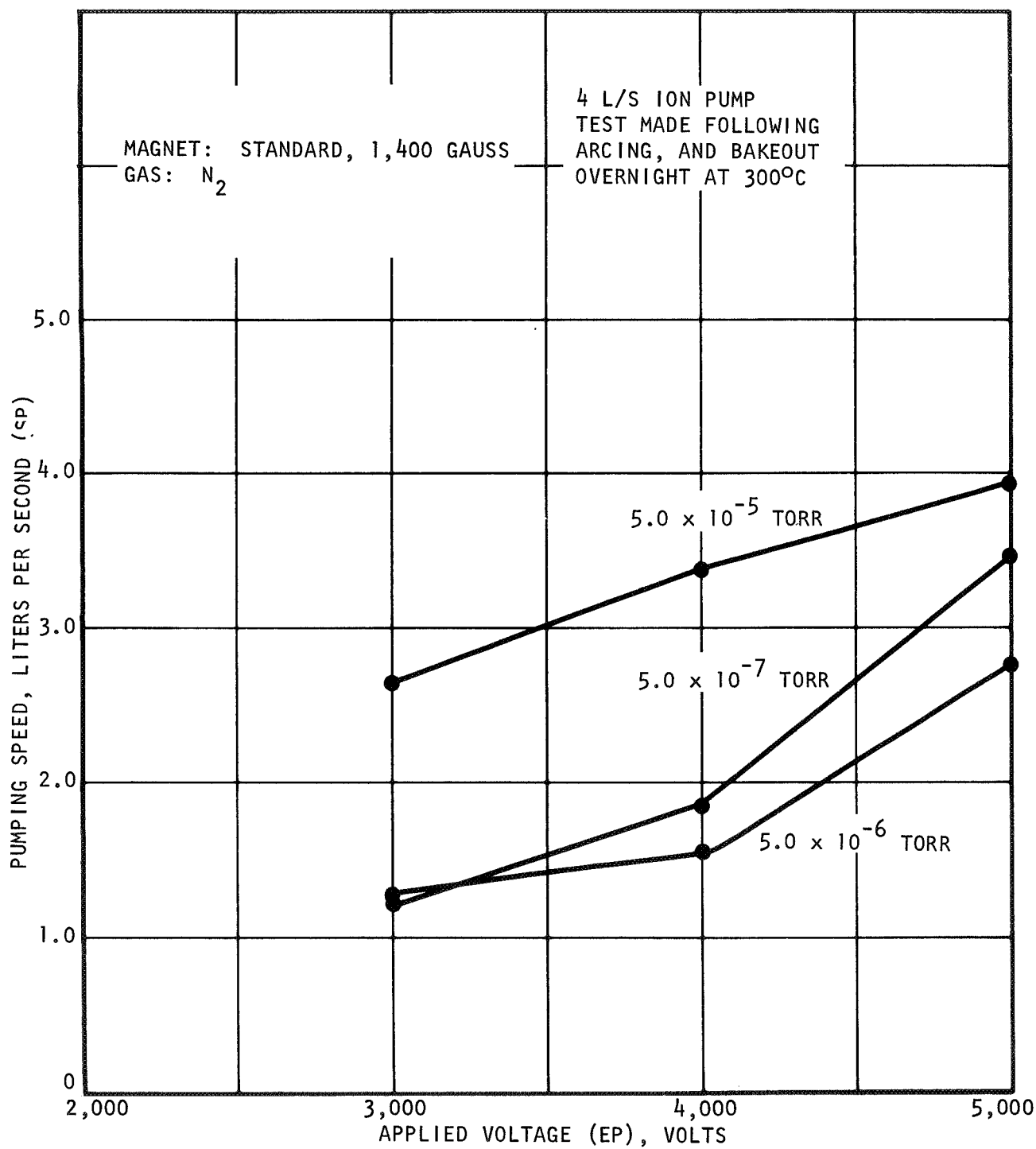


FIGURE 14.- Pumping Speed vs Voltage

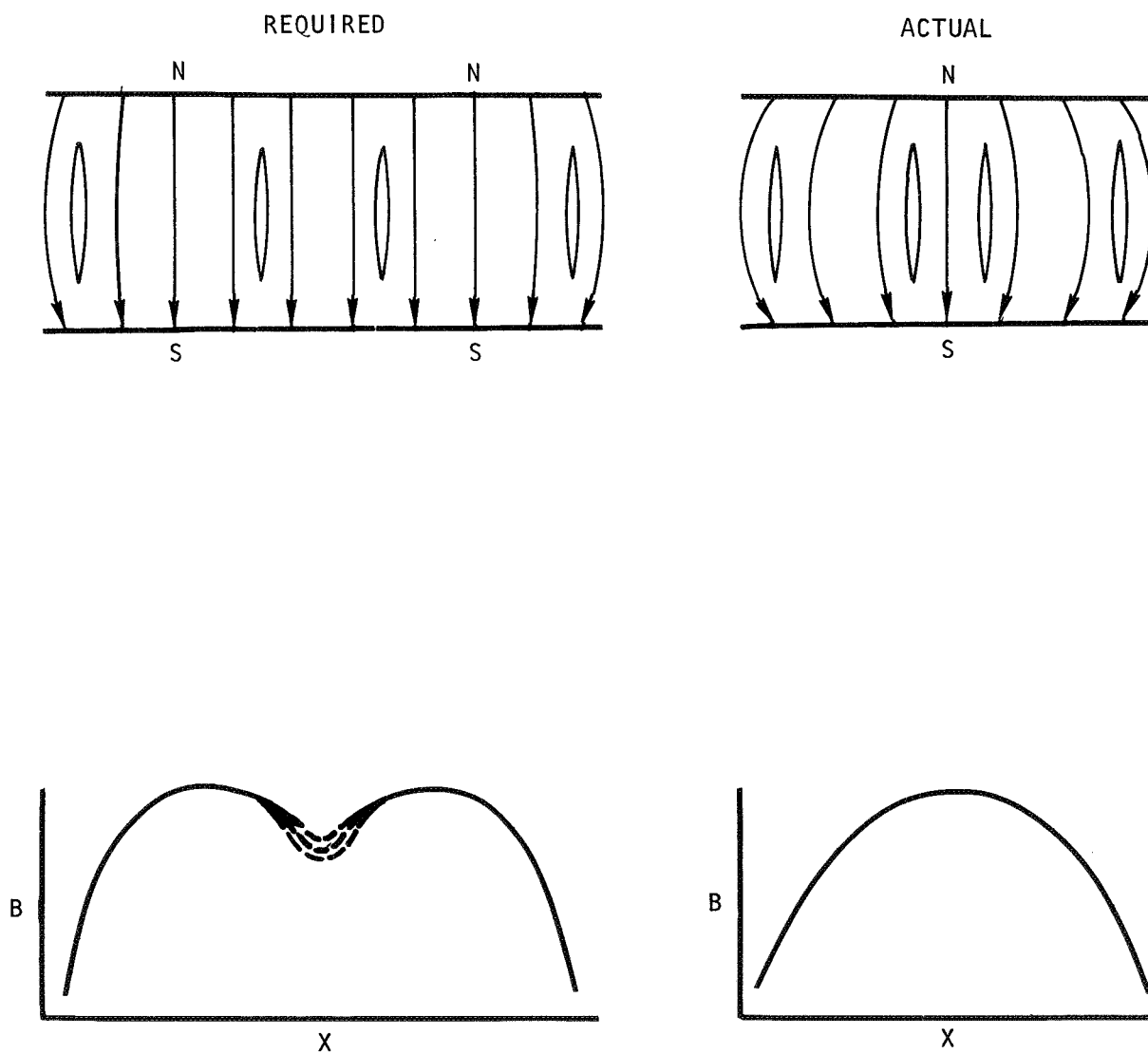


FIGURE 15.- Magnetic Field Geometry Comparison



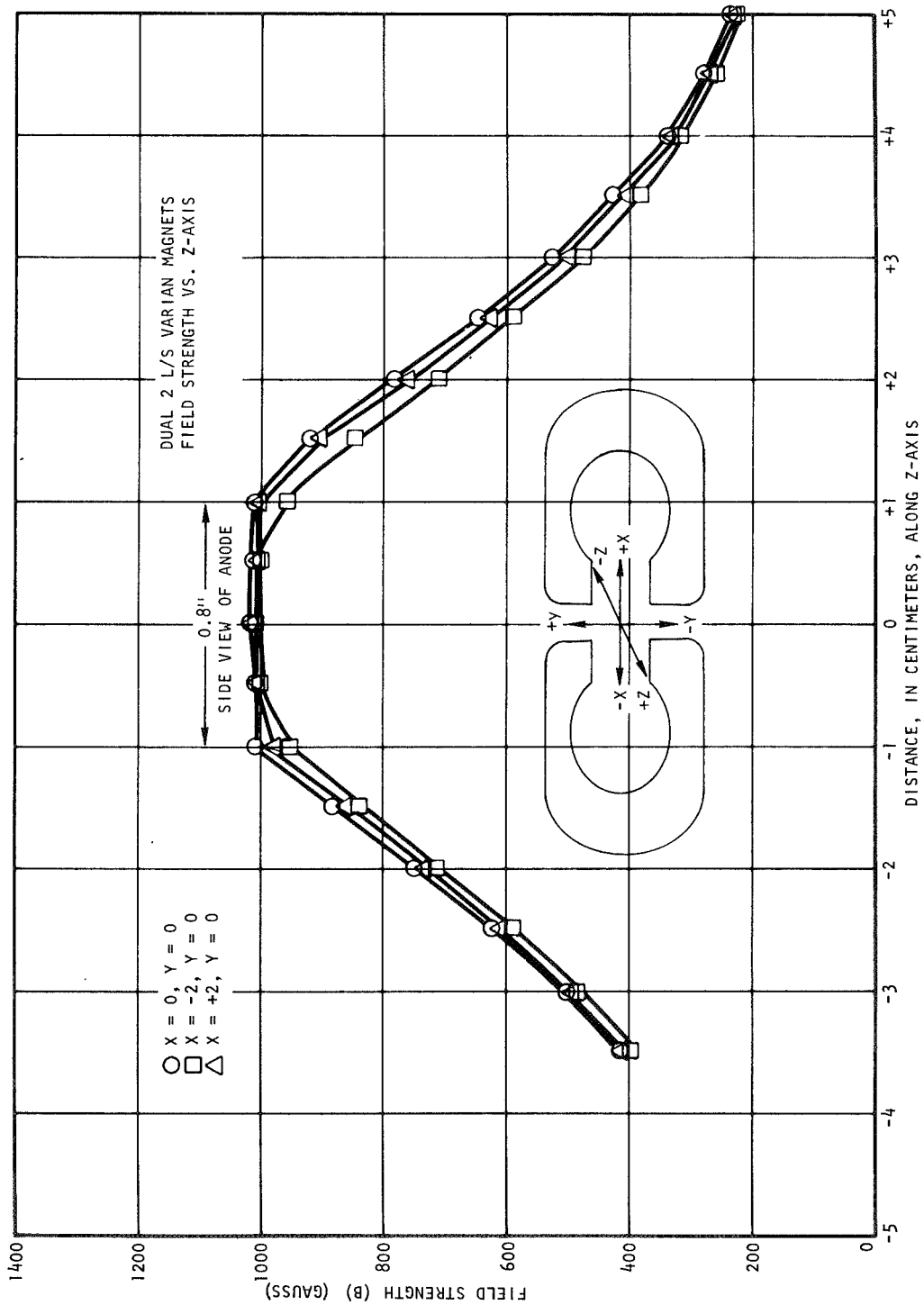


FIGURE 16.- Magnetic Field Test Results (Z-Axis)

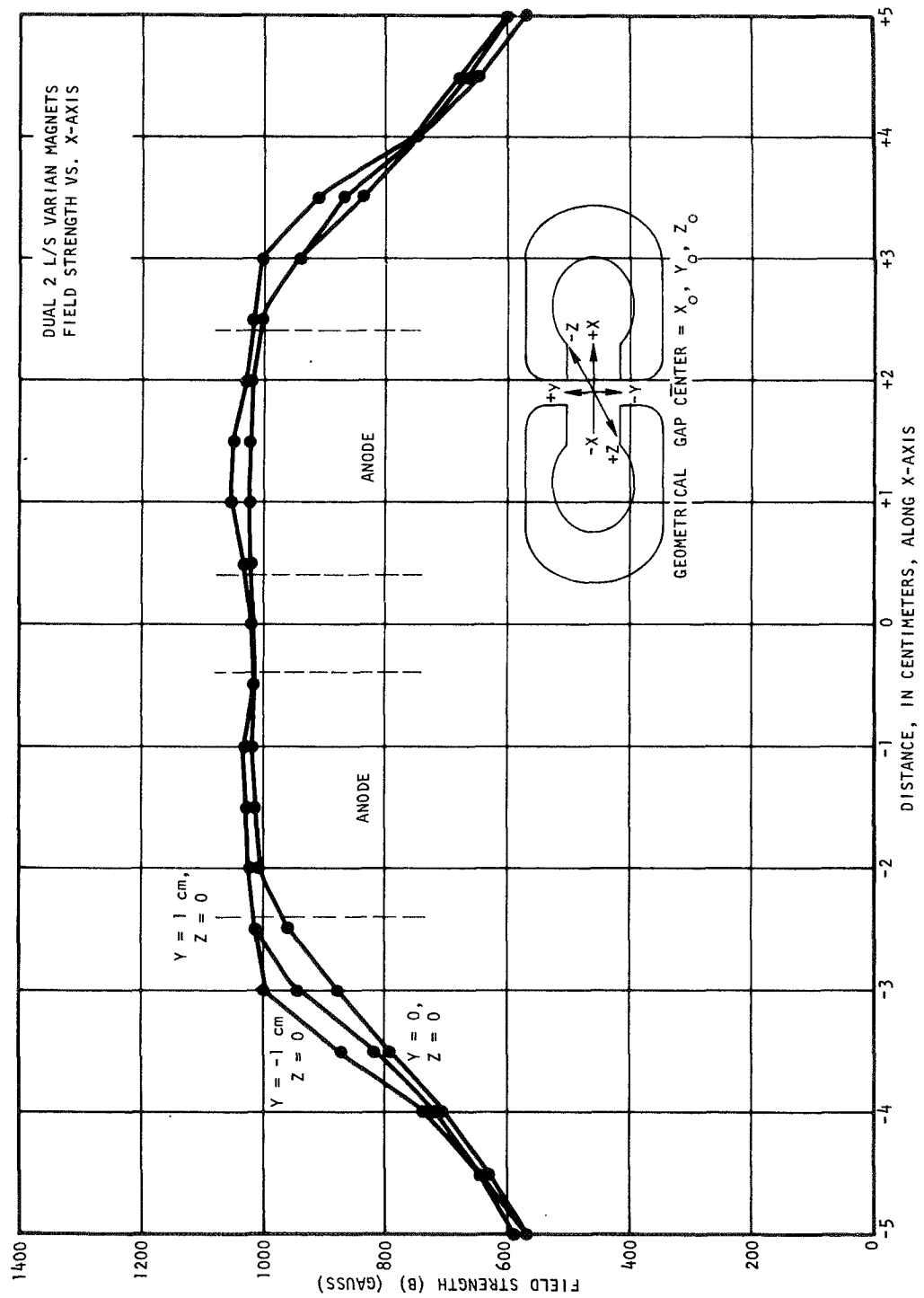


FIGURE 17.- Magnetic Field Test Results (X-Axis)

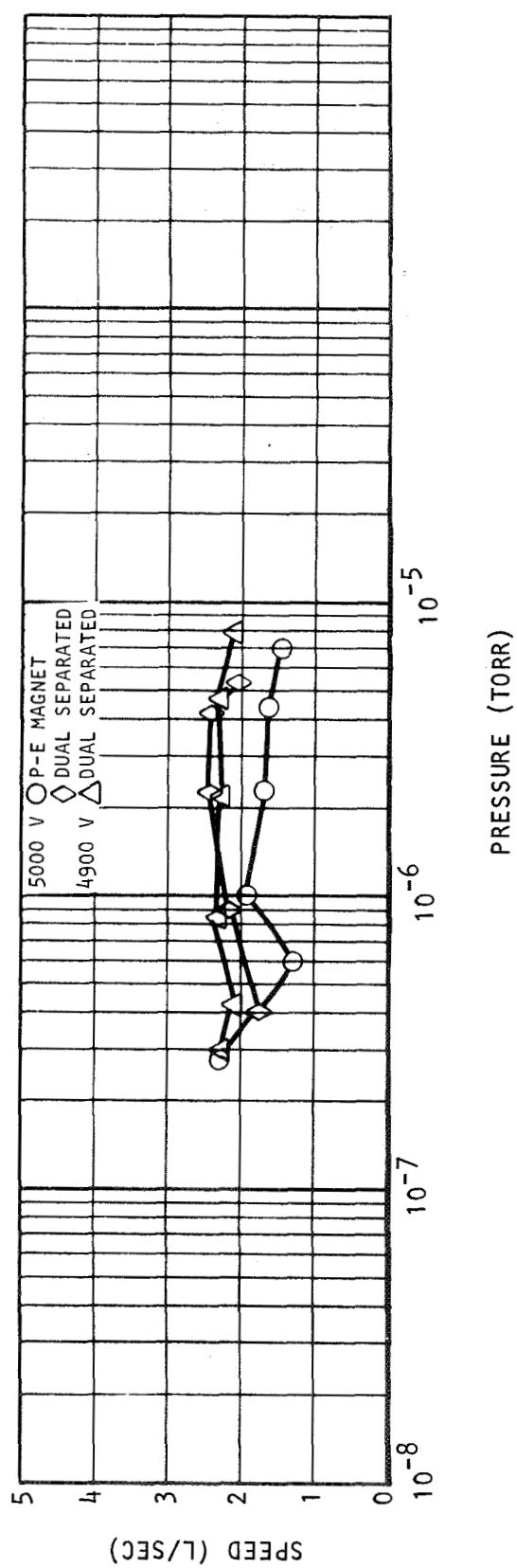
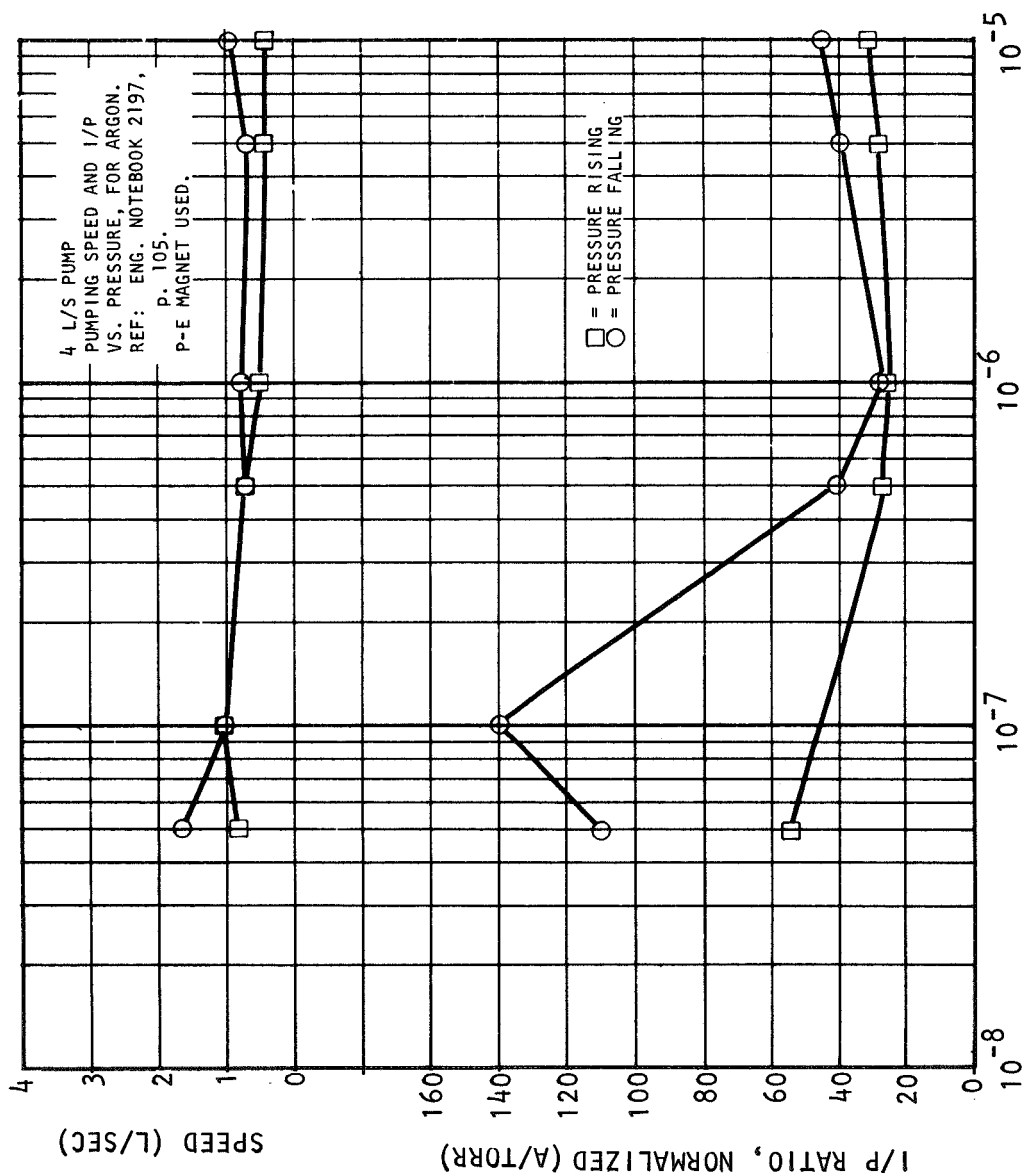


FIGURE 18.- Dual Separated vs Single Magnet



PRESSURE (P<sub>1</sub>) AT PUMP ENTRANCE (TORR)

FIGURE 19.- Argon Pumping Speed

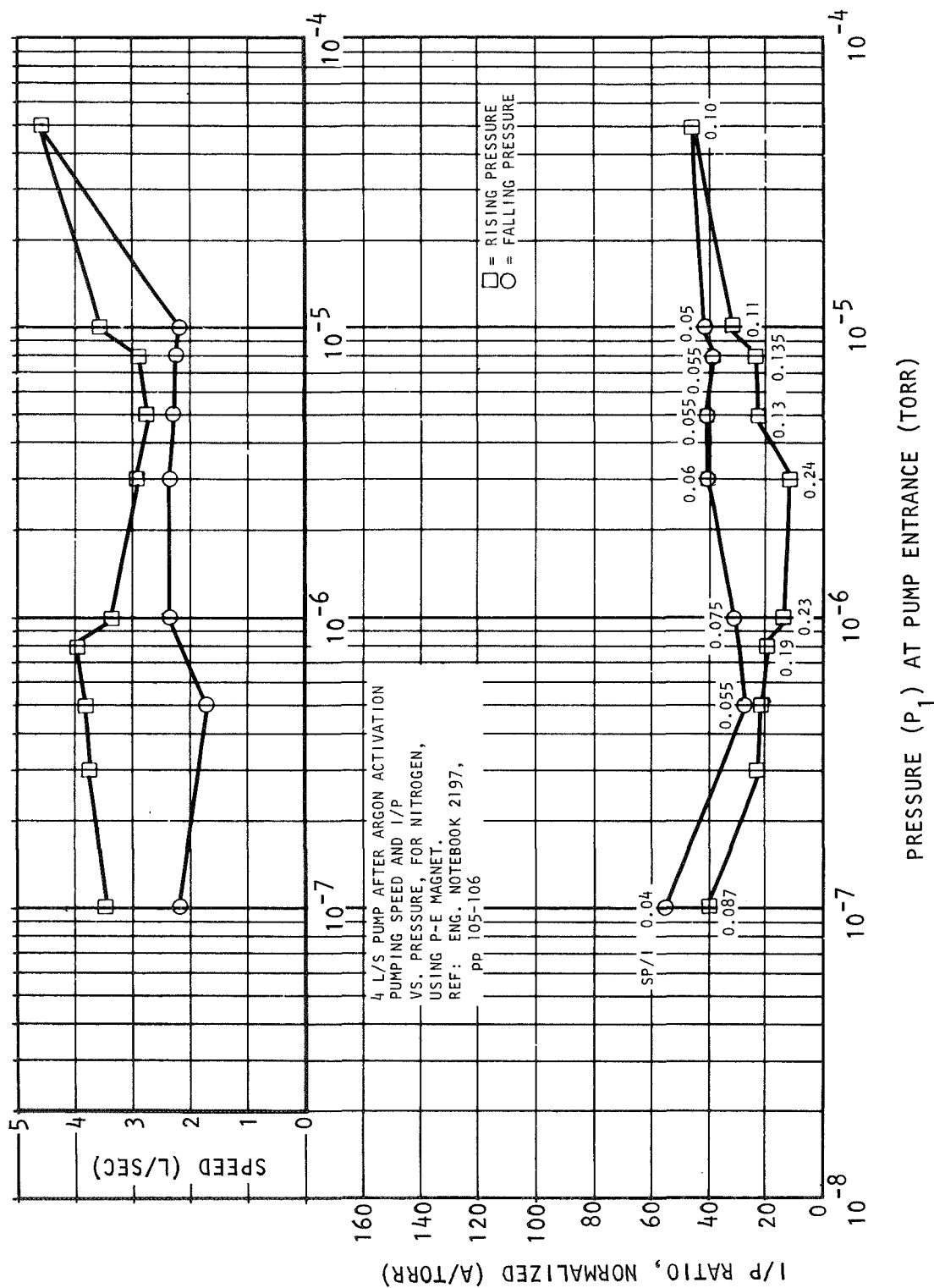


FIGURE 20.- 4 l/sec Pump After Argon Activation

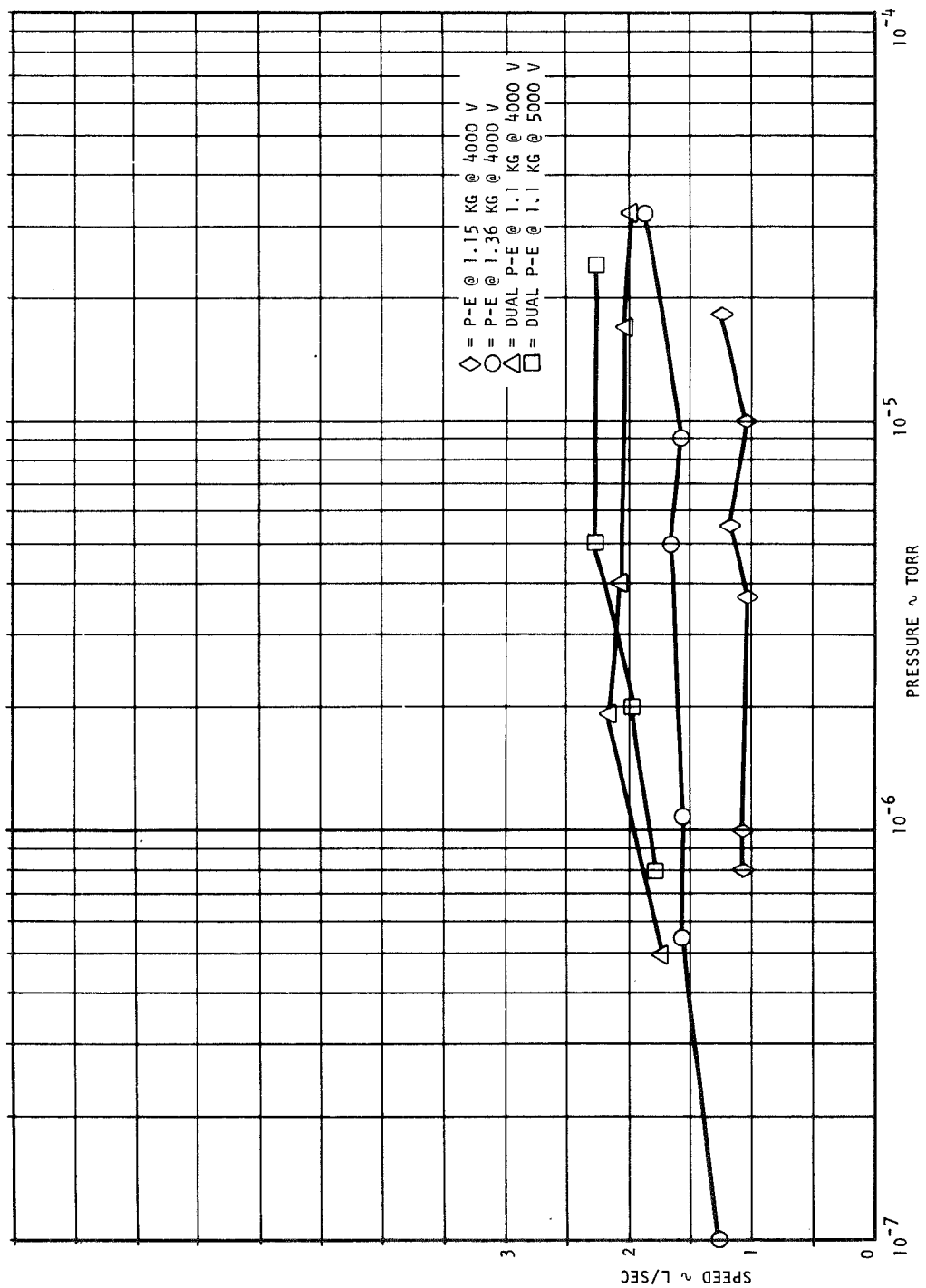


FIGURE 21.- Geometry and Field Strength Affect Test Data

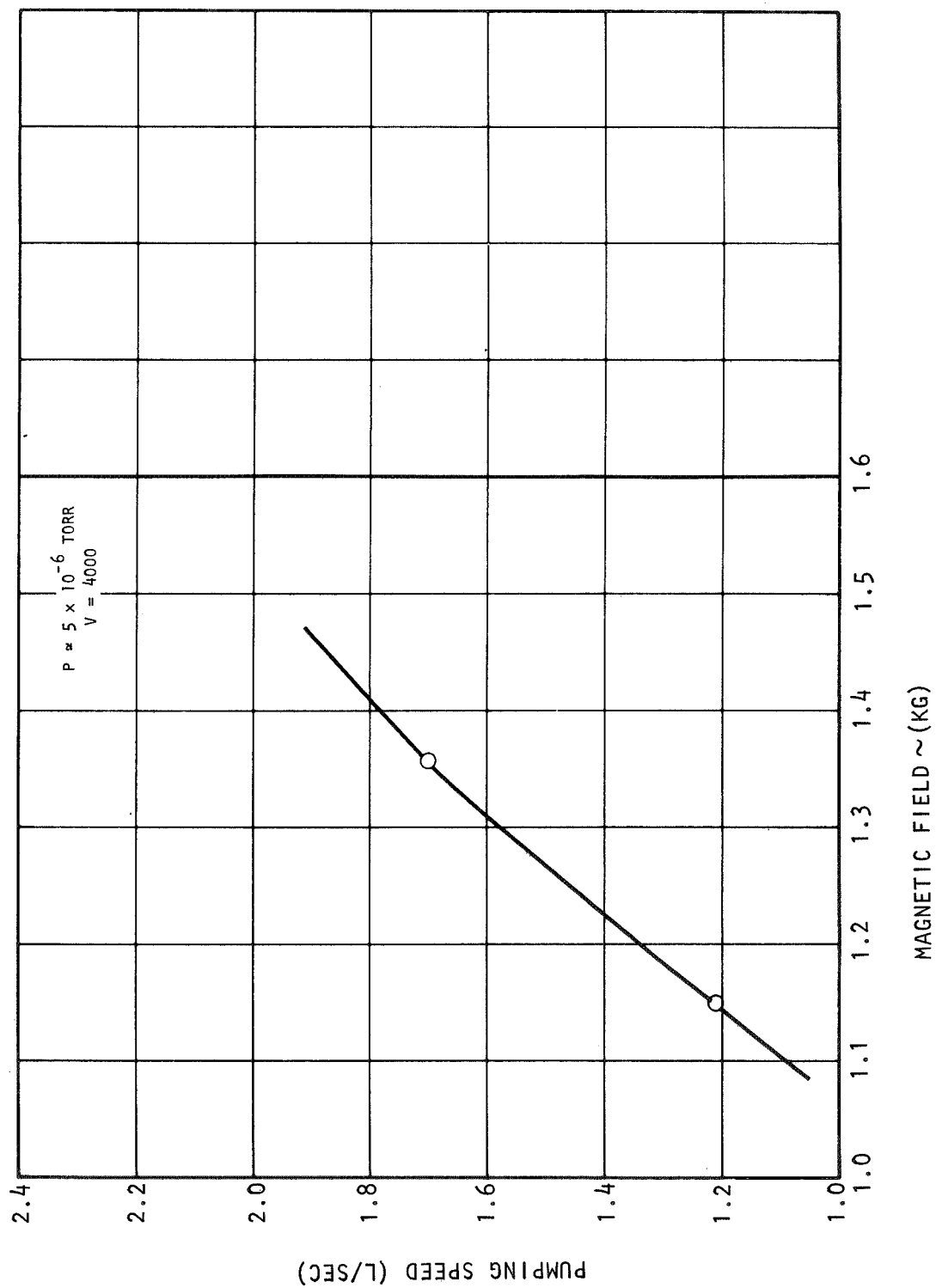


FIGURE 22.- Pumping Speed vs Field Strength

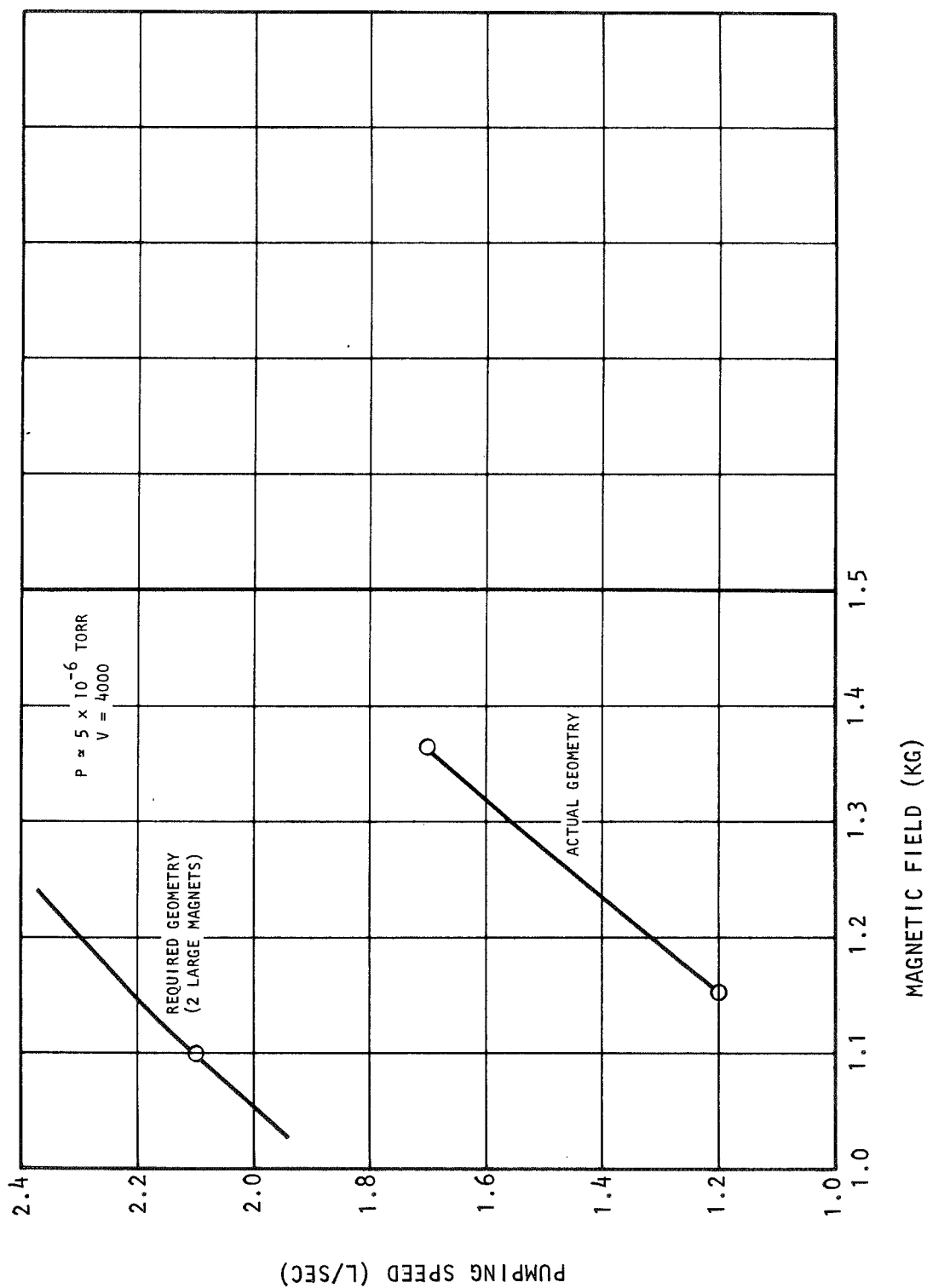


FIGURE 23.- Pumping Speed vs Field Geometry



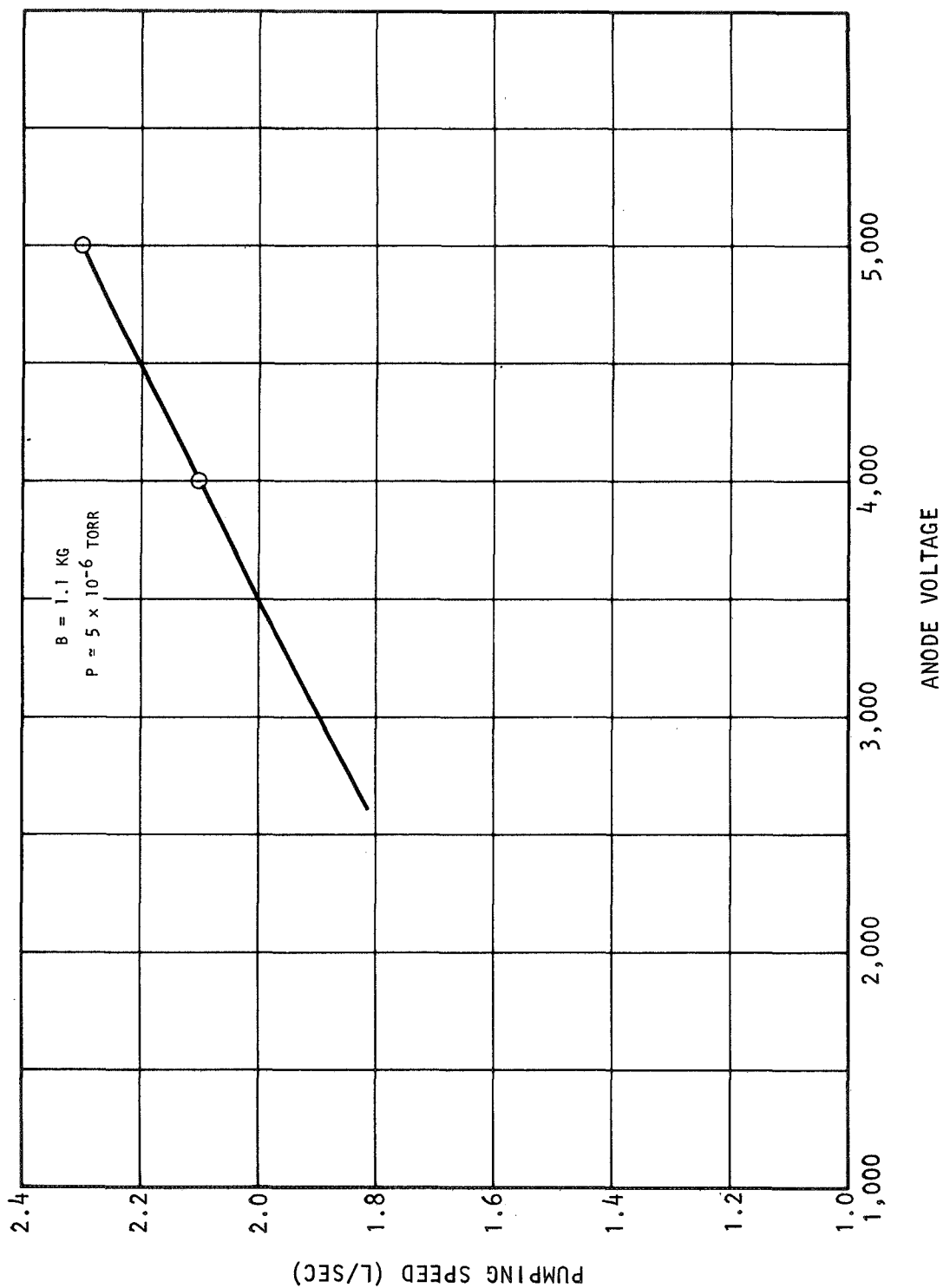


FIGURE 24.- Pumping Speed vs Voltage

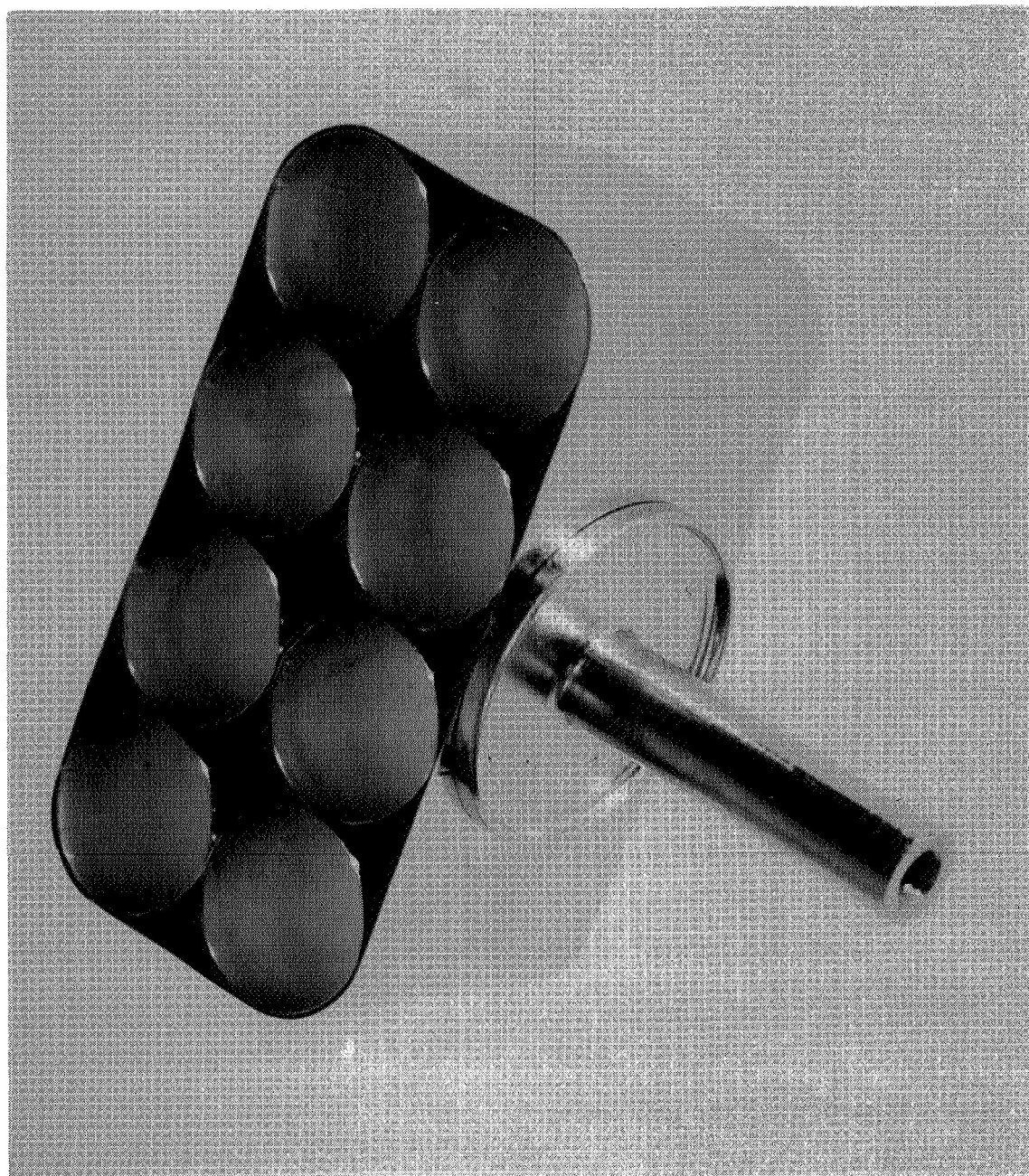
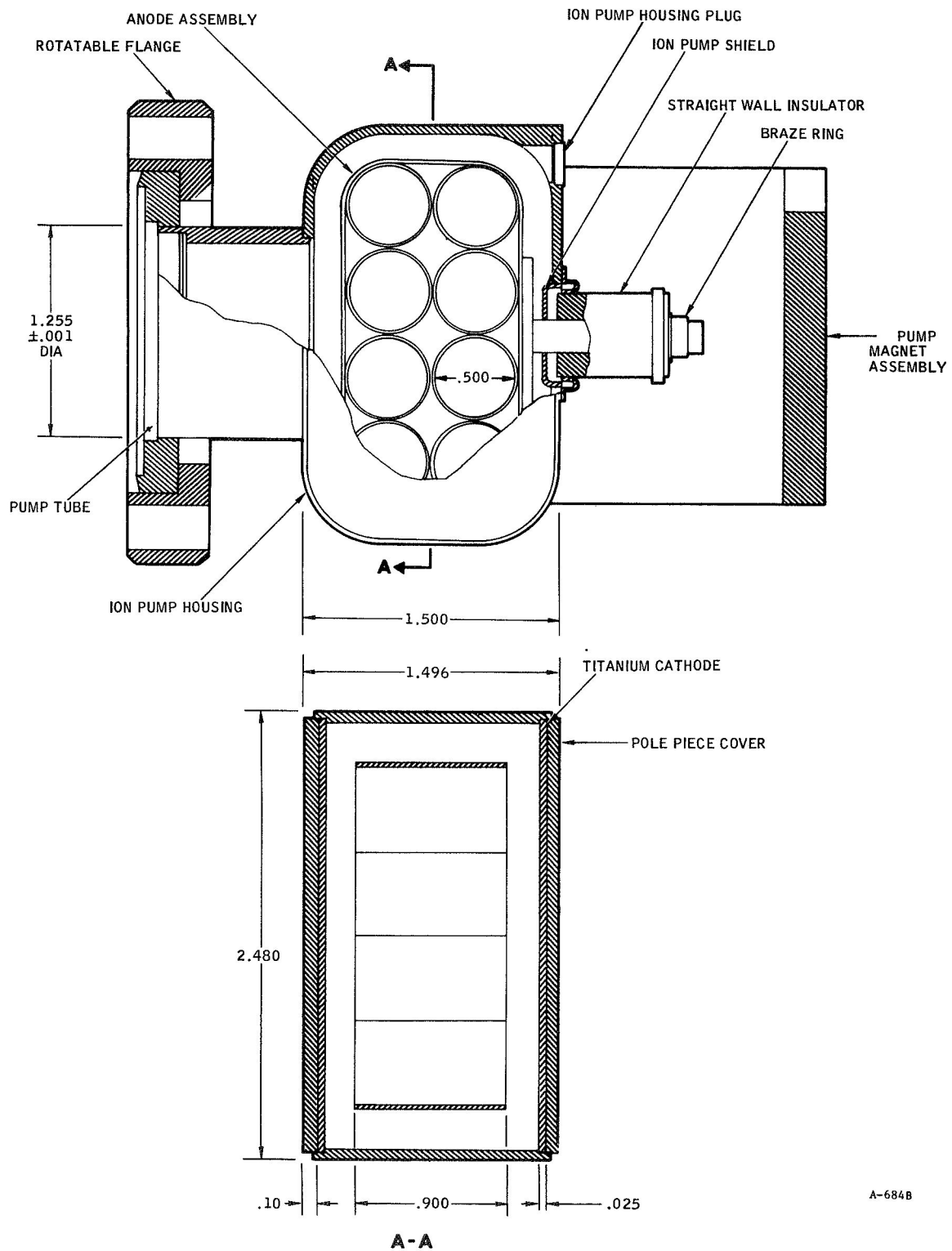


FIGURE 25.- Anode Assembly of Eight-Cell Ion Pump



A-684B

FIGURE 26.- Eight-Cell Prototype Ion Pump

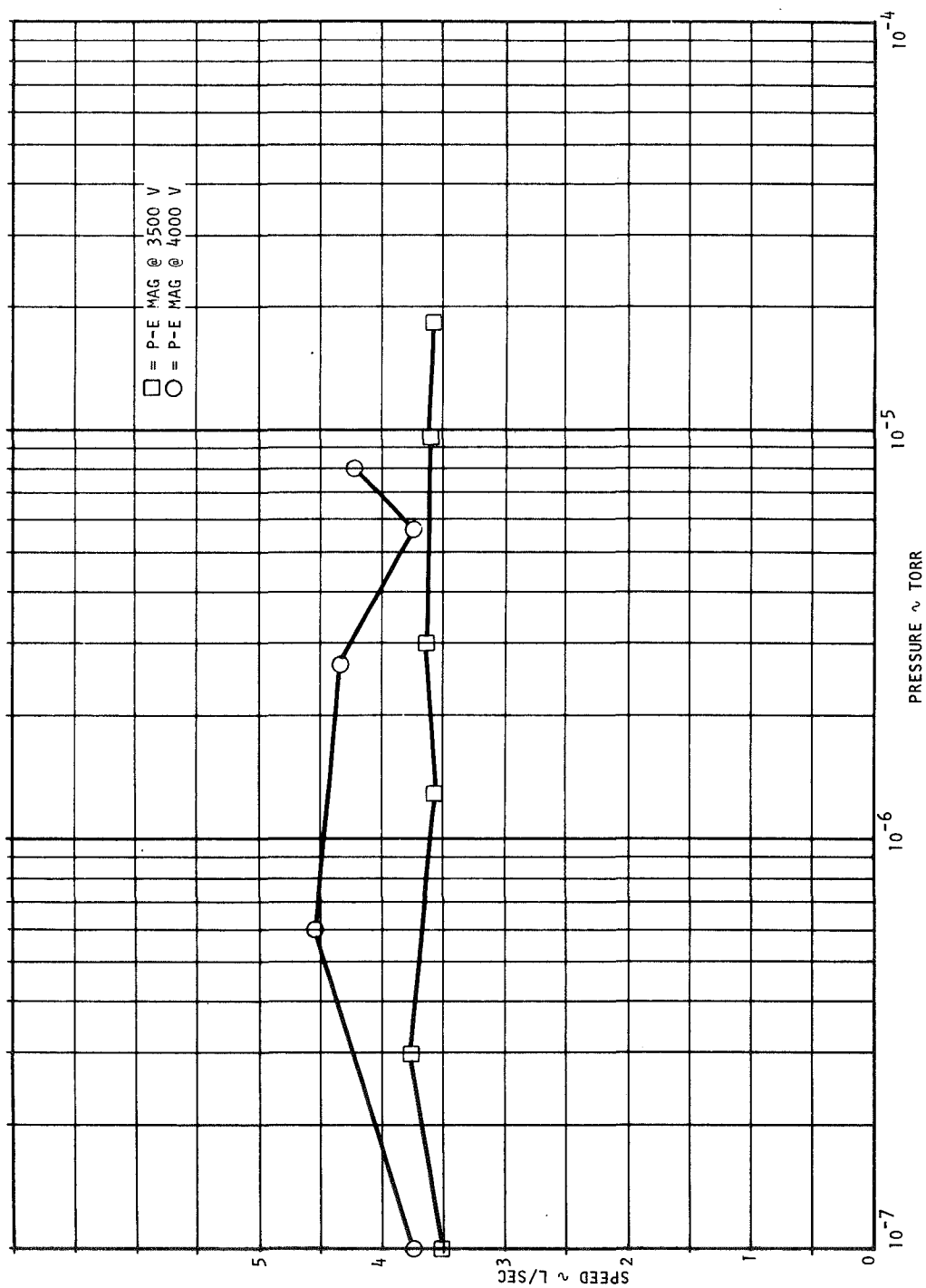


FIGURE 27.- Pumping Speed vs Pressure Eight-Cell Pump (Prototype)

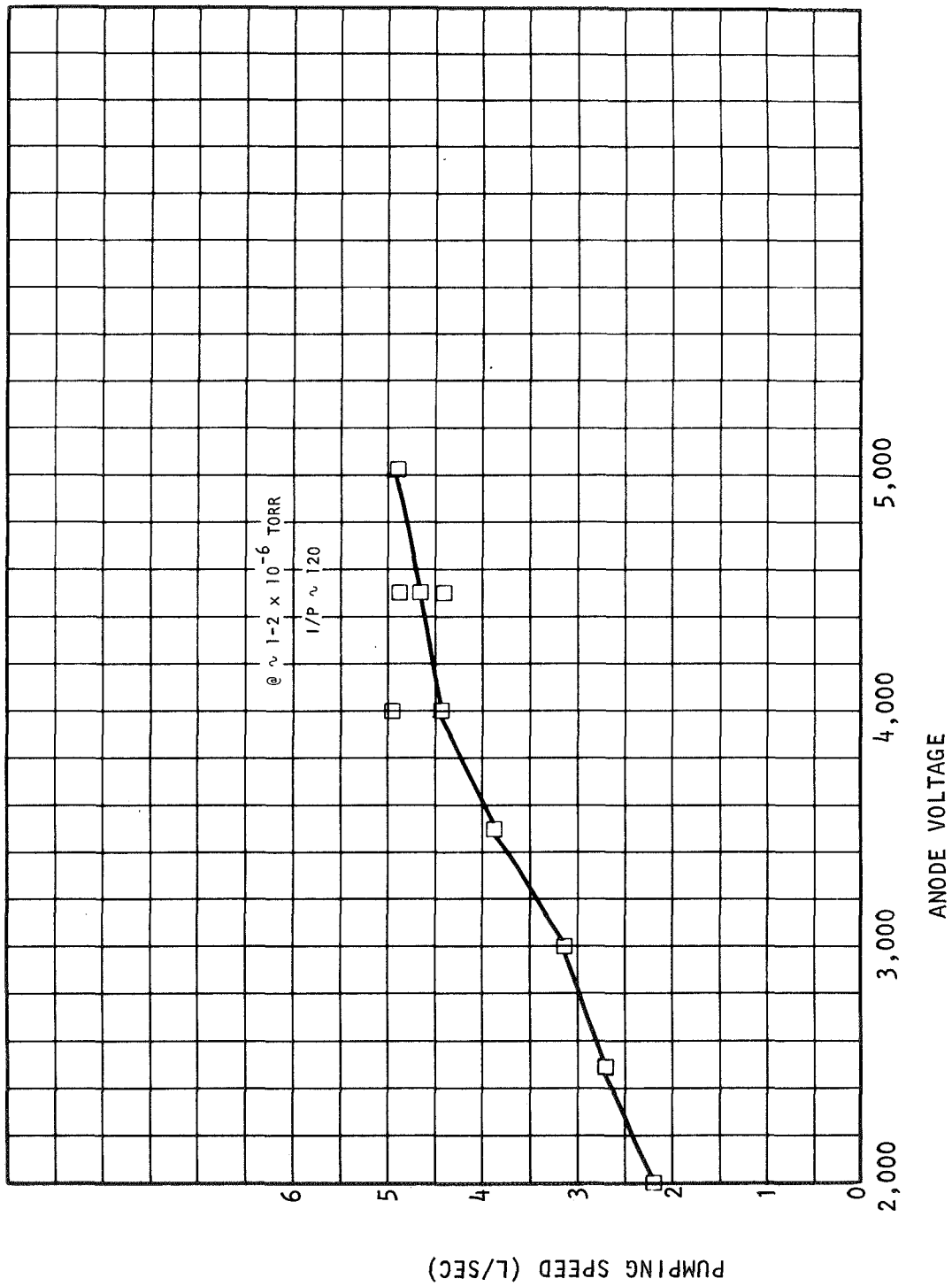


FIGURE 28.- Pumping Speed vs Voltage Eight-Cell Prototype

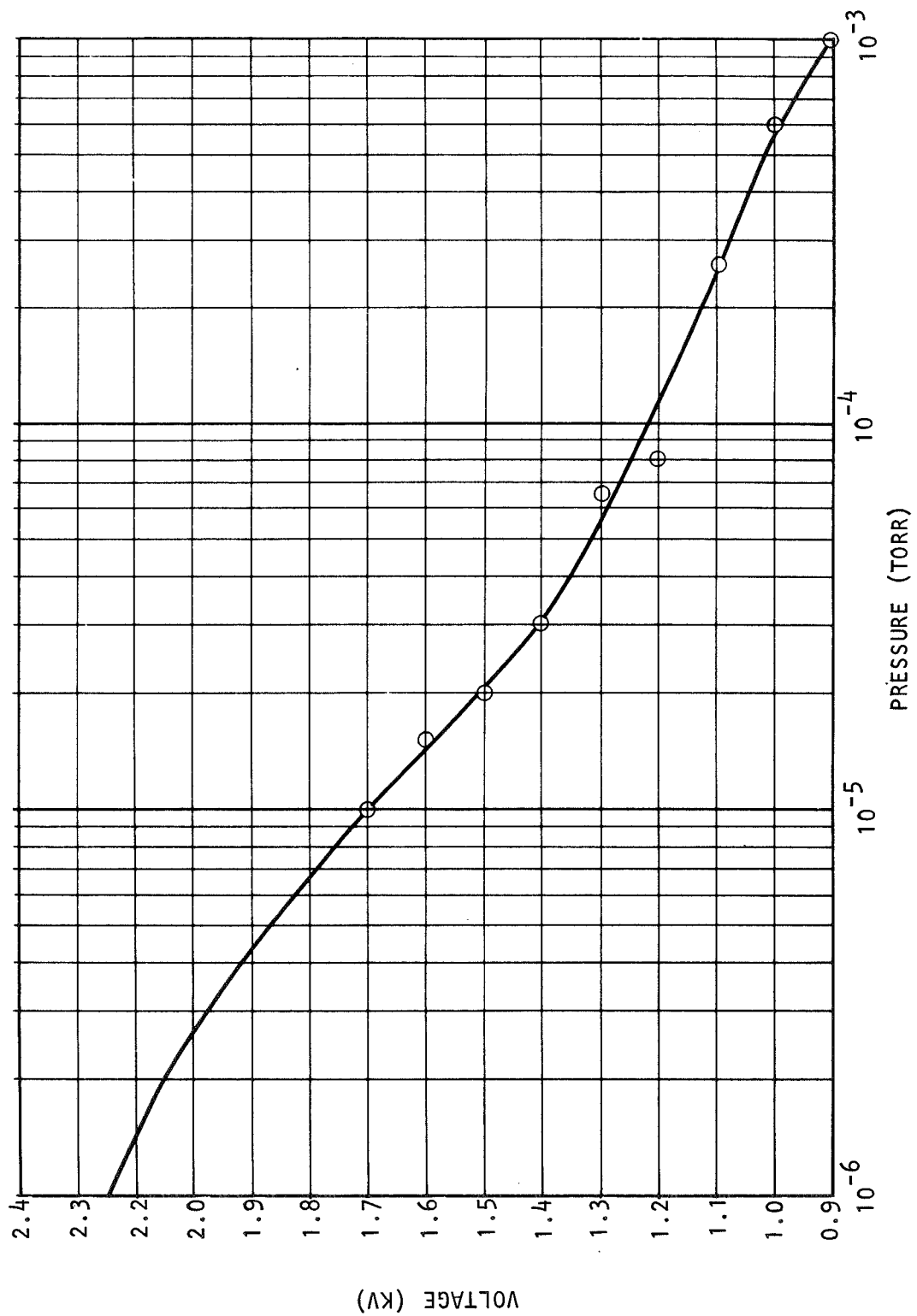


FIGURE 29.- Pressure vs Starting Voltage

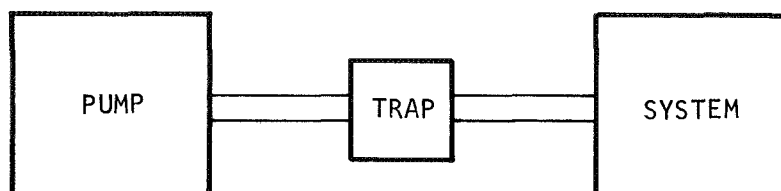


FIGURE 30.- Mechanical Pumping and Foreline Trap

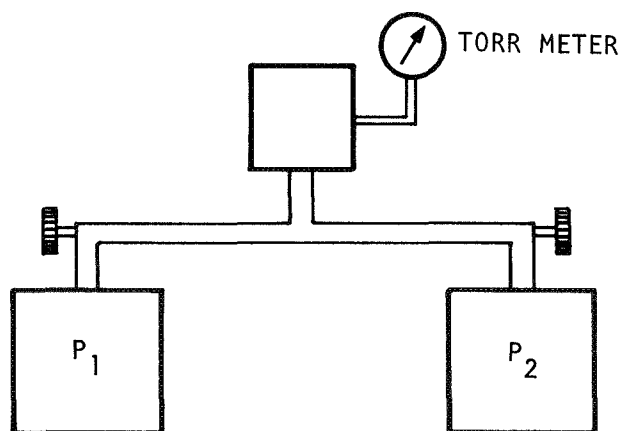


FIGURE 31.- Cryo-Sorption Pumping  
(Pumps at Room Temperature 25°C)

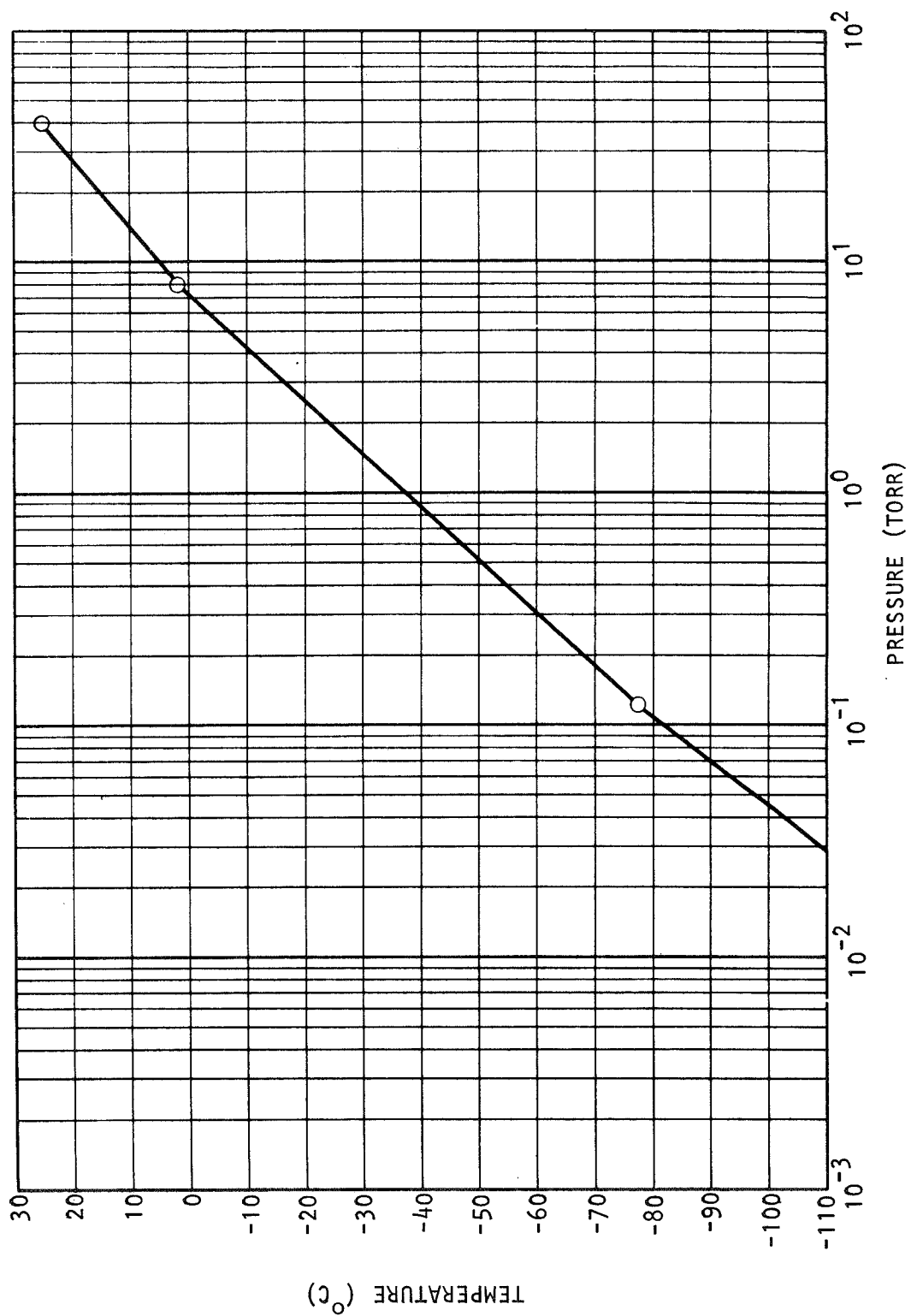


FIGURE 32.- Lowest Pressure vs Temperature Cascading Cryopumps (Two)



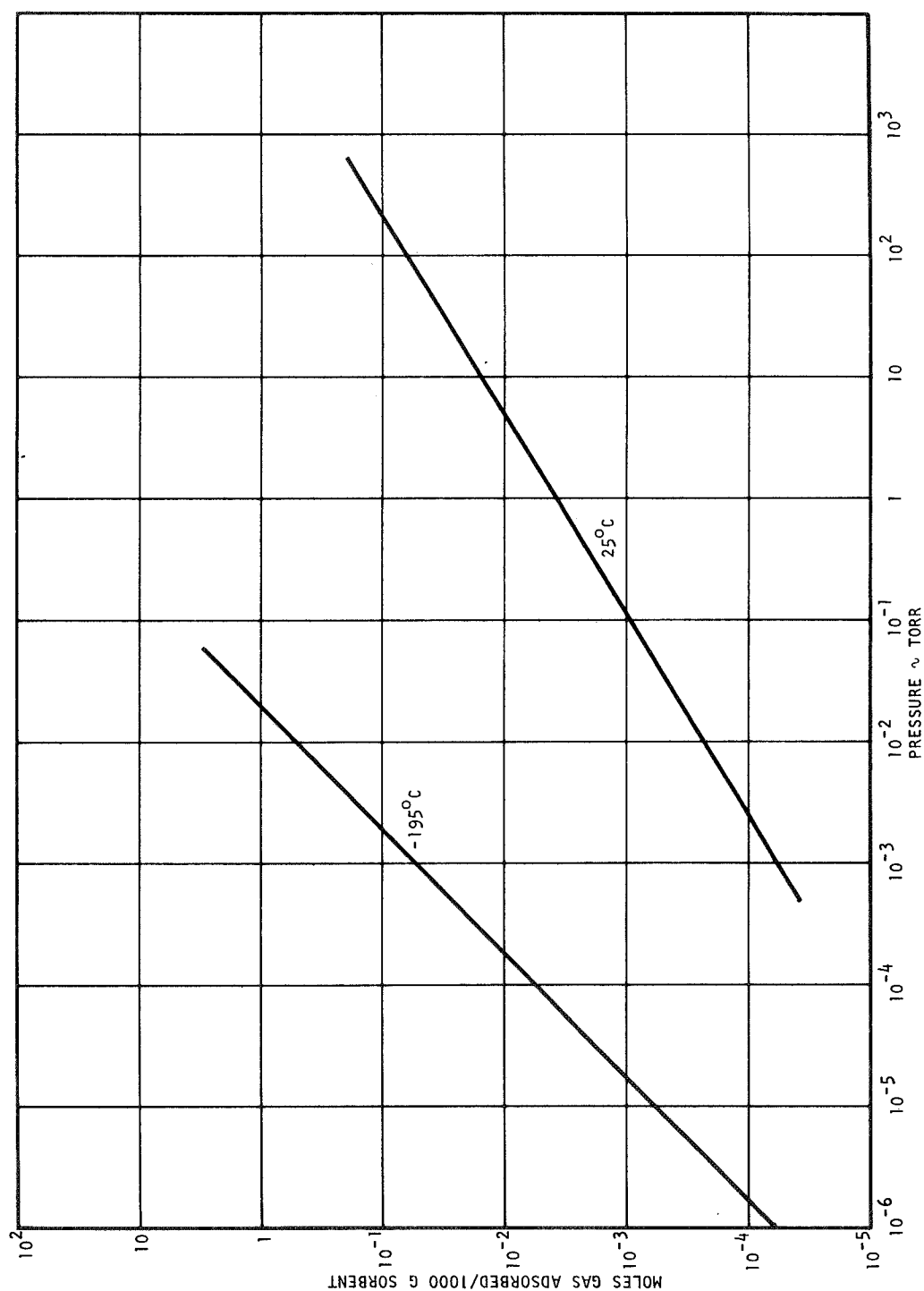


FIGURE 33.- Typical Adsorption Isotherms

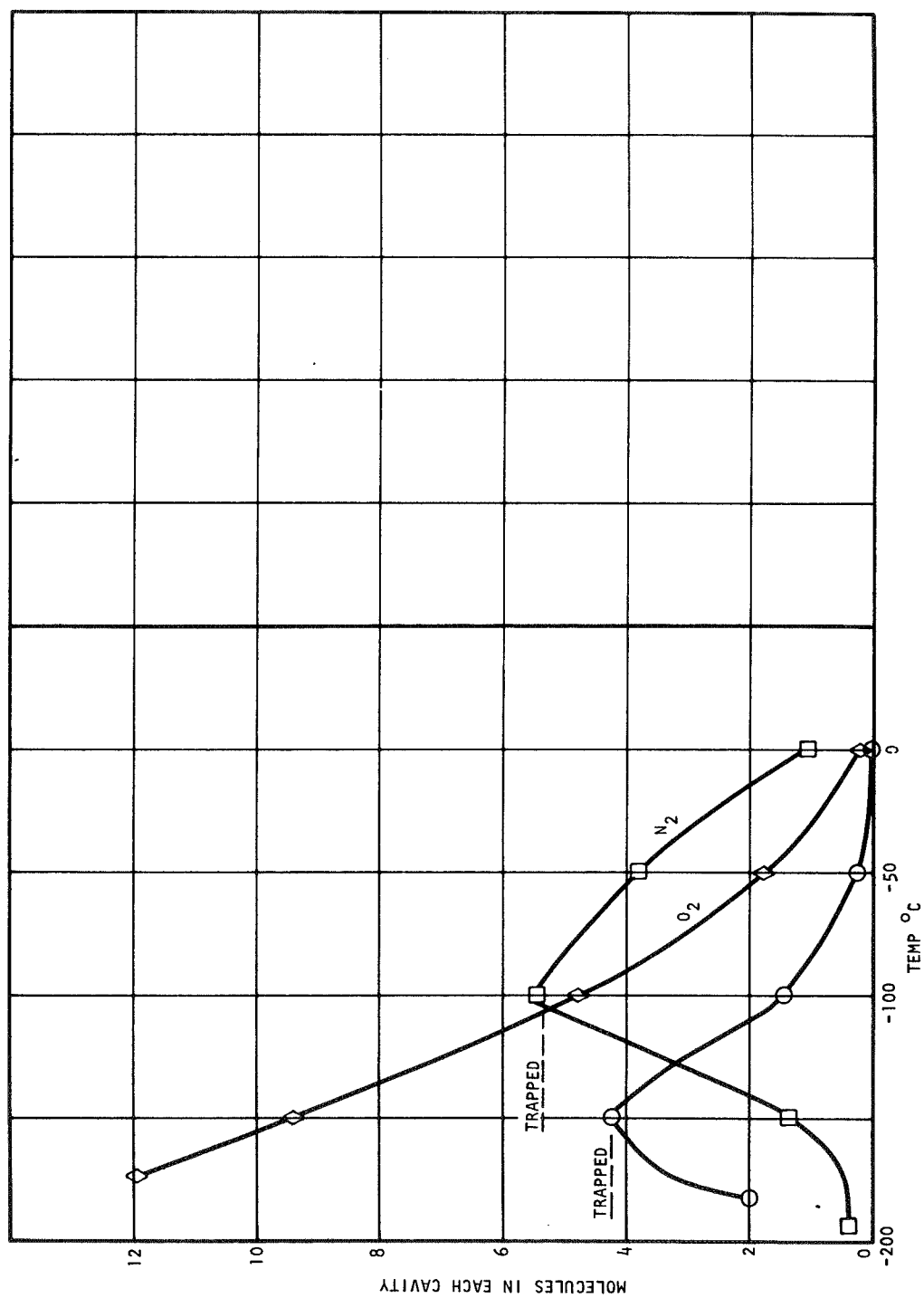


FIGURE 34.- Sorption of Gases by Zeolites vs Temperature (Typical)